

Article

Dissolved Carbon Concentrations and Emission Fluxes in Rivers and Lakes of Central Asia (Sayan–Altai Mountain Region, Tyva)

Arisiya A. Byzaakay ^{1,2}, Larisa G. Kolesnichenko ¹, Iury Ia. Kolesnichenko ¹ , Aldynay O. Khovalyg ², Tatyana V. Raudina ¹ , Anatoly S. Prokushkin ³ , Inna V. Lushchaeva ¹, Zoia N. Kvasnikova ⁴, Sergey N. Vorobyev ¹ , Oleg S. Pokrovsky ^{5,6,*}  and Sergey Kirpotin ¹

- ¹ Bio-Clim-Land Centre of Excellence, Tomsk State University, Lenin Avenue, 36, 634050 Tomsk, Russia; arisiy@inbox.ru (A.A.B.); klg77777@mail.ru (L.G.K.); vancansywork@mail.ru (I.I.K.); tanya_raud@mail.ru (T.V.R.); luschaeva@mail.ru (I.V.L.); soil@green.tsu.ru (S.N.V.); kirp@mail.tsu.ru (S.K.)
- ² Research Organization Department, Tuvan State University, Lenina Street, 36, 667000 Kyzyl, Russia; aldyn@mail.ru
- ³ V.N. Sukachev Institute of Forest SB RAS, Akademgorodok 50/28, 660036 Krasnoyarsk, Russia; prokushkin@ksc.krasn.ru
- ⁴ Geology and Geography Faculty, Tomsk State University, Lenin Avenue, 36, 634050 Tomsk, Russia; zojkwas@rambler.ru
- ⁵ Geosciences and Environment Toulouse, UMR 5563 CNRS, 31400 Toulouse, France
- ⁶ N. Laverov Federal Center for Integrated Arctic Research of the Ural Branch of the Russian Academy of Sciences, Northern Dvina Emb. 23, 163000 Arkhangelsk, Russia
- * Correspondence: oleg.pokrovsky@get.omp.eu; Tel.: +33-561332625

Abstract: The carbon (C) cycle in inland waters, including carbon concentrations in and carbon dioxide (CO₂) emissions from water surfaces, are at the forefront of biogeochemical studies, especially in regions strongly impacted by ongoing climate change. Towards a better understanding of C storage, transport and emission in Central Asian mountain regions, an area of knowledge that has been extremely poorly studied until now, here, we carried out systematic measurements of dissolved C and CO₂ emissions in rivers and lakes located along a macrotransect of various natural landscapes in the Sayan–Altai mountain region, from the high mountains of the Western Sayan in the northwest of Tyva to the arid (dry) steppes and semideserts in the intermountain basins in the southeast of Tyva on the border with Mongolia. New data on major hydrochemical parameters and CO₂ fluxes (fCO₂) gathered by floating chambers and dissolved organic and inorganic carbon (DOC and DIC, respectively) concentrations collected over the four main hydrological seasons allowed us to assess the current C biogeochemical status of these water bodies in order to judge possible future changes under climate warming. We further tested the impact of permafrost, river watershed size, lake area and climate parameters as well as ‘internal’ biogeochemical drivers (pH, mineralization, organic matter quality and bacterial population) on CO₂ concentration and emissions in lakes and rivers of this region and compared them with available data from other subarctic and mountain settings. We found strong environmental control of the CO₂ pattern in the studied water bodies, with thermokarst lakes being drastically different from other lakes. In freshwater lakes, pCO₂ negatively correlated with O₂, whereas the water temperature exerted a positive impact on pCO₂ in large rivers. Overall, the large complexity of counteracting external and internal drivers of CO₂ exchange between the water surfaces and the atmosphere (CO₂-rich underground DIC influx and lateral soil and subsurface water; CO₂ production in the water column due to dissolved and particulate OC biodegradation; CO₂ uptake by aquatic biota) precluded establishing simple causalities between a single environmental parameter and the fCO₂ of rivers and lakes. The season-averaged CO₂ emission flux from the rivers of Tyva measured in this study was comparable, with some uncertainty, to the C uptake fluxes from terrestrial ecosystems of the region, which were assessed in other works.

Keywords: carbon; concentration; CO₂; emission; rivers; lakes; biogeochemical cycle; Central Asia; Altai–Sayan Mountains



Citation: Byzaakay, A.A.; Kolesnichenko, L.G.; Kolesnichenko, I.I.; Khovalyg, A.O.; Raudina, T.V.; Prokushkin, A.S.; Lushchaeva, I.V.; Kvasnikova, Z.N.; Vorobyev, S.N.; Pokrovsky, O.S.; et al. Dissolved Carbon Concentrations and Emission Fluxes in Rivers and Lakes of Central Asia (Sayan–Altai Mountain Region, Tyva). *Water* **2023**, *15*, 3411. <https://doi.org/10.3390/w15193411>

Academic Editor: Junhong Bai

Received: 3 September 2023

Revised: 20 September 2023

Accepted: 23 September 2023

Published: 28 September 2023



Copyright: © 2023 by the authors. Licensee MDPI, Basel, Switzerland. This article is an open access article distributed under the terms and conditions of the Creative Commons Attribution (CC BY) license (<https://creativecommons.org/licenses/by/4.0/>).

1. Introduction

The carbon (C) cycle in inland waters, including the dissolved and particulate concentrations of carbon and the carbon dioxide (CO₂) emissions, are at the forefront of biogeochemical studies, especially in the regions most sensitive to ongoing climate change such as boreal and subarctic zones [1–10] or the tropical/equatorial belt [11–14]. In contrast to these numerous works, C storage, transport and emission in central continental, mountain and arid regions remain strongly understudied, due either to limited access and logistics or to the still underestimated potential role of these remote territories in C cycling in inland waters. This is especially true for the Central Asian mountain system encompassing the Tibet, Himalaya, Pamir, Altai and Sayan regions. Exceptions are the thorough works on DOC, DIC and POC fluxes in the Himalayan rivers [15–17] and C concentrations and fluxes in thermokarst lakes of the Tibetan Plateau [18–23]. However, the northern part of the Central Asian Mountain System remains virtually unexplored from the viewpoint of hydrochemistry and carbon balance in its rivers and lakes.

The Altai–Sayan Mountain system is a specific inland region of the northern part of Central Asia which covers the territory of four countries: Russia, Mongolia, China and Kazakhstan [24]. In Russia, it is located within the Tyva Republic, Altai Republic, Buryatia, Khakassia, and Krasnoyarsk Krai. It is characterized by a high degree of continentality and aridity as well as the highest level of endemism under a huge variety of ecosystems and landscapes, many of which are vulnerable to climatic changes [25]. The water bodies such as rivers and lakes are of particular importance for the sustainability, ecosystem services and conservation of the biodiversity of this arid region [26–31]. The particular interest in the Altai–Sayan region is that currently occurring climate changes in this territory contradict existing world models and forecasts. In particular, in the Tyva Republic, our group reported the first ever observed occurrence of the natural phenomenon of ‘greening’ or afforestation of steppes and bare sands [32,33]. This finding contrasts with a number of prediction models that stipulated further progressive drying of the arid Altai and Sayan regions (ASR), such as Khakassia, Tyva and Mongolia [34,35]. The other existing assessments of future climates in arid regions of Eurasia also predict an increase in aridity and even propose the propagation of desertification in the steppe regions [36–38]. For instance, in the Tyva Republic, the areal extension of steppe ecosystems, including dry steppes, is predicted to increase by 20–65%, whereas in semideserts, the projected increase is predicted to be several hundred percent more compared to their current extent [24].

In contrast to the above-mentioned predictions, some other studies suggest an increase in the climatic instability, such as drastic transformation of the main atmospheric circulation, in the south Siberia regions and at the border with Central Asia, which could lead to a decrease in the role of atmospheric transport from Atlantic regions, resulting in the blocking of anticyclones and an increase in meridional atmospheric transport [39,40]. This process, in turn, could cause many catastrophic weather events, such as the dramatic appearance of rainstorms, hurricanes and water floods, together leading to the progressive humidification of arid, previously dry regions [41]. Such catastrophic weather events have been observed over the last few years in Khakassia, Tuva and Mongolia [42–44].

It is clear that the ongoing climate changes can drastically impact the current hydrochemical, biogeochemical and hydrological status of the inland rivers and lakes of the region. For example, it is known that lakes at high altitudes and cold climates are particularly sensitive to global change [45,46] and modifications in carbon biogeochemistry, including the status of dissolved organic matter (DOM), and C emission fluxes may strongly alter the role of these lakes in the global C cycle [47–49]. Among the consequences of the progressive humidification of Central Asian arid regions under ongoing climate change, the treeline shift (greening of upland and advancement of treeline) can strongly affect the biogeochemical functioning of lakes, given that 15% of all lakes globally are located at elevations 500 m or more above sea level [50]. Further, existing paleo-reconstructions suggest that lake productivity [51] and biogeochemistry [52] are sensitive to changes in DOM input linked to treeline position. Therefore, thorough assessment of today’s status

of the C biogeochemical cycle (concentration, emission from the water surfaces) is necessary to be able to judge the possible future changes in Central Asian regions induced by climate instability.

Over the past decade, a few studies in this area addressed the hydrochemical [53–58], hydrological and hydrographic [59–61] status of the water bodies, including the balneological aspect of mineral springs [62–65]. There are also some studies conducted on the hydrochemistry of water bodies in adjacent regions of Mongolia [66]. However, the status of aquatic C and CO₂ emissions from the water surfaces of the Altai–Sayan region remain unknown. Towards filling this gap in knowledge, here, we assessed the concentration of dissolved organic and inorganic carbon and C emissions in lakes and rivers of the Tyva region by selecting large and small water bodies affected by permafrost to different degrees. A novel physico-geographical and climatic transect of inland water bodies, which we implemented in this study, extends from the northwest (the highlands of the western Sayan) to the southeast (the semideserts of the Ubsunur Depression on the border with Mongolia). This transect comprises a large variety of natural ecosystems and landscapes of the region, from glacial–nival high mountain belts to foothill taiga forests, intermountain basins with mixed herb and steppe ecosystems and dry semideserts. As a working hypothesis, we anticipated strong environmental control of C biogeochemical parameters of lakes and rivers, including climate, altitude, permafrost extent and size of the watershed as the main ‘external’ drivers of C concentration and emission. We also assessed the link between carbon parameters of the water bodies and possible ‘internal’ biogeochemical drivers (hydrochemical parameters) such as pH, mineralization, quality of dissolved organic matter and bacterial abundance. We tested these controls across the four main hydrological seasons (spring, summer, autumn and winter) in five lakes and 15 rivers of different sizes and landscape contexts.

2. Materials and Methods

2.1. Water Bodies of the Tyva Republic

We visited 20 water bodies during four hydrological seasons (autumn 2021–summer 2022), as shown in Figures 1 and 2. The main physico-geographical parameters of the rivers and lakes are listed in Tables 1 and 2 and are described in detail in the Appendix A. The Republic of Tyva is located in the Sayan–Altai Mountain region, between 50 and 53° N and between 88 and 99° E; the elevations range from 2000 to 500 m, creating a large variety of landscapes, from high-altitude belts to basins with steppes and semideserts. The climate of the region is continental, with cold, long winters and hot summers; the mean monthly temperatures range from –41 in January to +35 °C in July; the precipitation is low (115 to 350 mm y^{–1}), and about 70% of it falls during the warm season of the year [67].

During the period of our study, the temperature ranged from –28 °C to 21 °C, and the precipitation was equal to 322 and 144 mm during 2021 and 2022, respectively. (http://www.pogodaiklimat.ru/history/36096_2.htm, accessed on 23 September 2023). The water objects sampled in this work include numerous water bodies mainly belonging to the Yenisei River basin, whereas only a small number belonged to the closed basin of the Ubsunur basin.

The largest river flowing through the region is the Yenisei River, formed at the confluence of the Maly and Bolshoy Yenisei rivers. Most rivers of the Yenisei basin are of mountain origin, that is, they mainly have snow and groundwater feeding. The studied lakes are mostly drainless and mainly fed by groundwater, with the exception of Lake Chagytai [68,69]. We collected the water samples during four hydrological seasons, in autumn (24 October 2021–27 October 2021), winter (7 March 2022–11 March 2022), spring (18 May 2022–22 May 2022) and summer (19 August 2022–23 August 2022). During each season, we sampled 20 water bodies (15 rivers and five lakes), with 140 samples in total. These were selected according to the criterion of proximity to the weather stations throughout the climate/landscape macrotransect of Tyva.

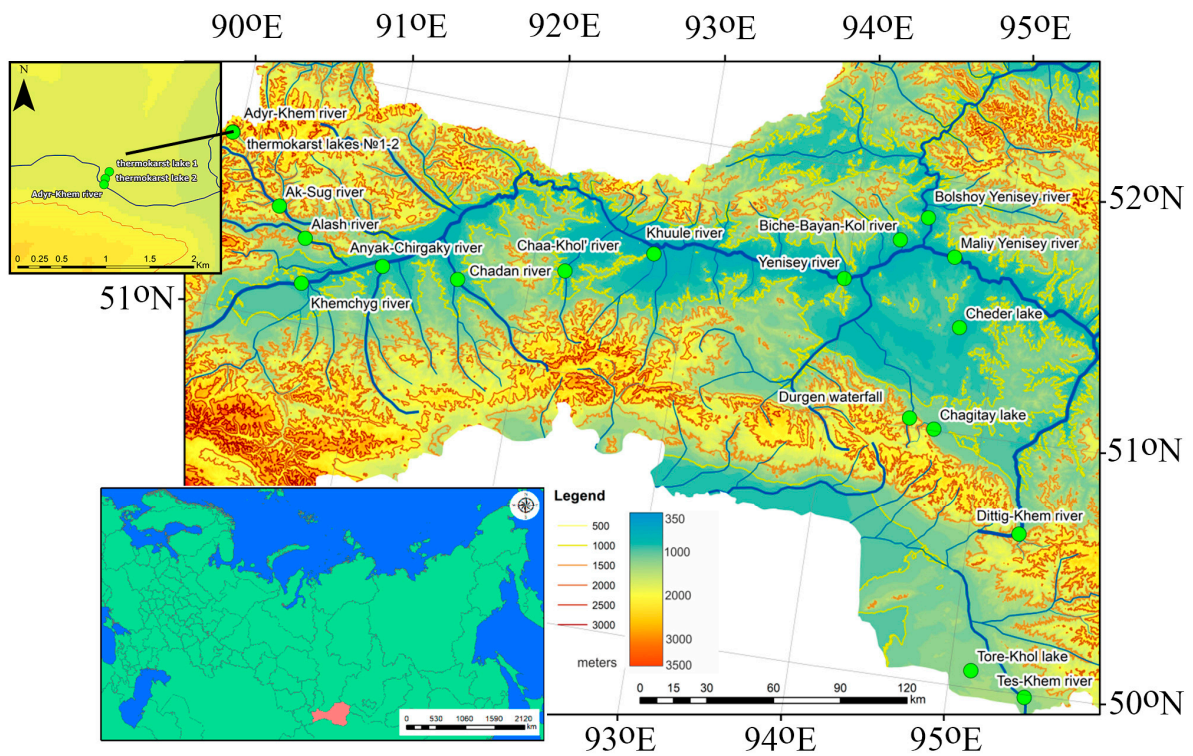


Figure 1. Location of research objects within the Sayan–Altai Mountain system (Central Asia).

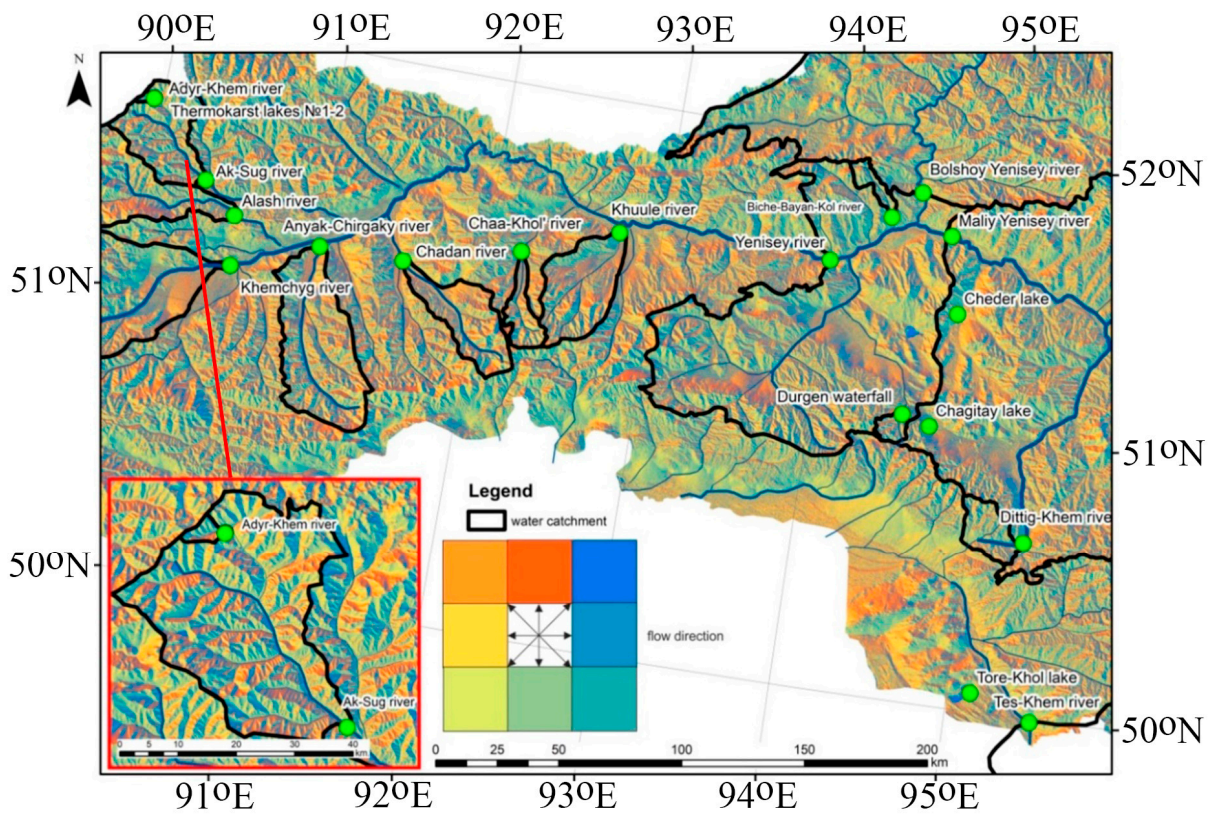


Figure 2. River catchments of the study region. The direction of water flow is shown by different colors.

Table 1. General information about the rivers sampled in this work.

Name	Flow Velocity m/s	Depth (m)	Length (km)	Average Discharge, m ³ /c	Catchment Area (km ²)	Height at the Samp-Ling Point, m	Average Catchment Height (m)	Slope of the Riverbed (m/km)	Location
Yenisei	0.25–2.6	2–3	3487	1020	102,806	650	1196	16.8	Ulug-Khem basin
Big Yenisei	1.4–2.4	1.5–4	605	594	57,766	630	1448	3.1	Todzhin-skaya basin; Kyzyl basin
Small Yenisei	1.8–2.3	1–2.4	563	411	36,395	636	1555	2.8	Sangilen Highlands; Ulugh-Khem basin
Tes-Hem	1.1–2.1	1–2.1	757	55.6	18,430	1067	1842	7.9	East Tannu-Ola
Hem-chik	-	0.75–2	320	102	3268	850	1923	14.4	Shapshal ridge; Khemchik basin
Alash	0.43	0.30–2	172	-	4741	920	2063	9.2	Alash Plateau
Ak–Sug	0.31	0.25–1	160	14	997.4	1150	1966	26.8	Alash Plateau
Chadan	-	-	98	-	881.5	800	1567	28.8	West Tannu-Ola
Durgen	0.54	0.66–1	93	-	121.7	1200	1751	42.3	The northern slope of East Tannu-Ola
Chaa-Hol	0.28	0.5–2	90	-	320.3	540	1694	43.1	The northern slope of the western Tannu-Ola
Huule (Torgalyg)	-	0.4–2	53	-	1090	535	1273	30.9	The northern slope of the Eastern Tannu-Ola; The Central Tuva basin
Anyyak-Chyrgaki	0.173	0.2–2	52	-	1859	800	1519	13.9	West Tannu-Ola
Dyttyg-Hem	-	0.2–0.8	34	-	426.9	1250	1710	36.3	Southern slope of East Tannu-Ola
Biche-Bayan-Kol	0.34	0.3–0.8	32	-	15.3	750	1222	26.0	Uyuk Ridge
Adyr-khem	0.17	0.5–2	8.25	-	8.25	1850	2076	66.2	Alash Plateau

Table 2. General information about the studied lakes [15].

Name	Depth (m)	Water Mirror Area, km ²	Type	Height (m)	Location
Tore-Khol	6–8 (max. 40 m)	68.8	Freshwater	1148	Ubsunur basin
Chagytai	17	28.6	Freshwater lake	1005	The foot of the northern slope of the Tannu-Ola ridge
Cheder	1.5–2	4.3	Salt lake	706	South of the Tuva basin, a drainless depression
Thermokarst 1	4	0.3	Thermokarst lake	1850	Alash Plateau
Thermokarst 2	5	0.1	Thermokarst lake	1850	Alash Plateau

2.2. Analytical Methods

The list of measured parameters included temperature, pH, electrical conductivity (E.C.) and concentration of dissolved gases (CO₂ and O₂), dissolved organic (DOC) and inorganic carbon (DIC), optical properties of organic matter, as well as CO₂ emission flux from the water surface. Dissolved oxygen, pH, electrical conductivity and temperature were measured in situ using an EXO2 multiparameter probe and a WTW Multi 3320 multimeter. The measurement of pCO₂ in water was carried out in situ using the GM70 data logger Vaisala®. The pCO₂ was measured in situ by an infrared gas analyzer (IRGA, GMT222, Vaisala, Finland) [70]. The sensor was enclosed in a semipermeable membrane and placed

directly into the surface water (30–50 cm depth), where it was allowed to equilibrate for approximately 30 min. The sensors were calibrated against standard gas mixtures (0, 800, 3000, 8000 ppm) before and after the sampling. Following calibration, results were corrected using water temperature and barometric pressure.

Carbon dioxide emissions from the water surface were measured by direct floating chamber method using SensAir sensors. We used a freely drifting chamber (30 cm diameter, covered with aluminum tape). The CO₂ accumulation rate inside the chamber was recorded continuously at 5 sec intervals for 5–10 min and used to compute (by linear regression if $R^2 > 0.75$) CO₂ flux and k_{CO_2} following Kuhn et al., 2018 [71]. For all calculations, the CO₂ air–water equilibrium was calculated assuming an air concentration of 400 ppm. Further details of pCO₂ and fCO₂ measurements in rivers and lakes of adjacent regions are provided elsewhere [1,72–75].

River and lake water was collected from the surface (depth 0.5 m) in a precleaned polypropylene container with a capacity of 1 L and immediately filtered through nitrate-cellulose filters (<0.45 microns, Sartorius Minisart High Flow). DOC and DIC were measured in the BIO-GEO-CLIM Laboratory (TSU) using a total organic carbon analyzer of the TOC-LCSN series, Shimadzu, with an uncertainty of 2%. As an indicator of the quality of DOM, we measured visual and UV absorbance using spectrophotometry (Agilent Cary 300 spectrophotometer). These measurements allowed for the assessment of spectral slopes ($S_{290-350}$, $S_{275-295}$, $S_{350-400}$); the slope ratio (S_R) is useful for approximating the molecular weight of DOM and the degree of its aromaticity. The relative amount of aromatic compounds was assessed via specific UV absorbance ($SUVA_{254}$). The weight-average molecular weight index (WAMW) of DOM, which reflects the degree of polymerization, was quantified using the absorbance at 280 nm. Finally, the humification index was characterized using the ratio of absorbance at 250 and 400 nm (the E2:E4 ratio).

Total bacterial cell (TBC) concentration was measured after sample fixation in glutaraldehyde (in the field immediately after collection) using flow cytometry (Guava® EasyCyte™ systems, Merck, Rahway, NJ, USA). Cells were stained using 1 µL of 10 times diluted SYBR GREEN solution (10,000×, Merck), added to 250 µL of each sample before analysis. Particles were identified as cells based on green fluorescence and forward scatter.

To build the maps, the DAICHI satellite (ALOS) survey with a resolution of 30 m² was used together with the 3D Analysis module in the ArcGIS environment. To delineate the catchments of the studied rivers, the Flow Direction module was used in the ArcGIS environment, which calculates flow lines based on data on the heights of nearby points.

Carbon concentrations and fluxes measured in rivers and lakes were tested for normality using a Shapiro–Wilk test. In case the data were not normally distributed, we used nonparametric statistics. Comparisons of dissolved C parameters between seasons and groups of the water bodies were conducted using a nonparametric Mann–Whitney test at a significance level of 0.05. For comparison of unpaired data, a nonparametric H-criterion Kruskal–Wallis test was used to assess the differences between sites. The Pearson rank order correlation coefficient ($p < 0.05$) was used to determine the relationship between CO₂ concentrations and flux and the main hydrochemical parameters of the water column, which are considered as potential drivers (pH, O₂, water temperature, electrical conductivity, DOC, DIC and total bacterial number). Boxplots of median, IQR and outliers were constructed for visualization of the differences between different seasons and groups of rivers or lakes.

3. Results

3.1. Major Hydrochemical Parameters

The values of pH varied significantly during different seasons of the year ($F = 11.31$, $p = 0.000$, Figure 3a) and between the two major types of the water bodies—lakes and rivers ($F = 10.67$, $p = 0.000$; Figure 3b,c). The electrical conductivity (E.C., µS cm⁻¹) in the studied water bodies varied widely and increased in the following order: thermokarst lakes

$(29 \pm 22) < \text{large rivers } (172 \pm 97) < \text{small rivers } (207 \pm 121) < \text{freshwater lakes } (534 \pm 252) < \text{salt lake } (54,600 \pm 24,380)$.

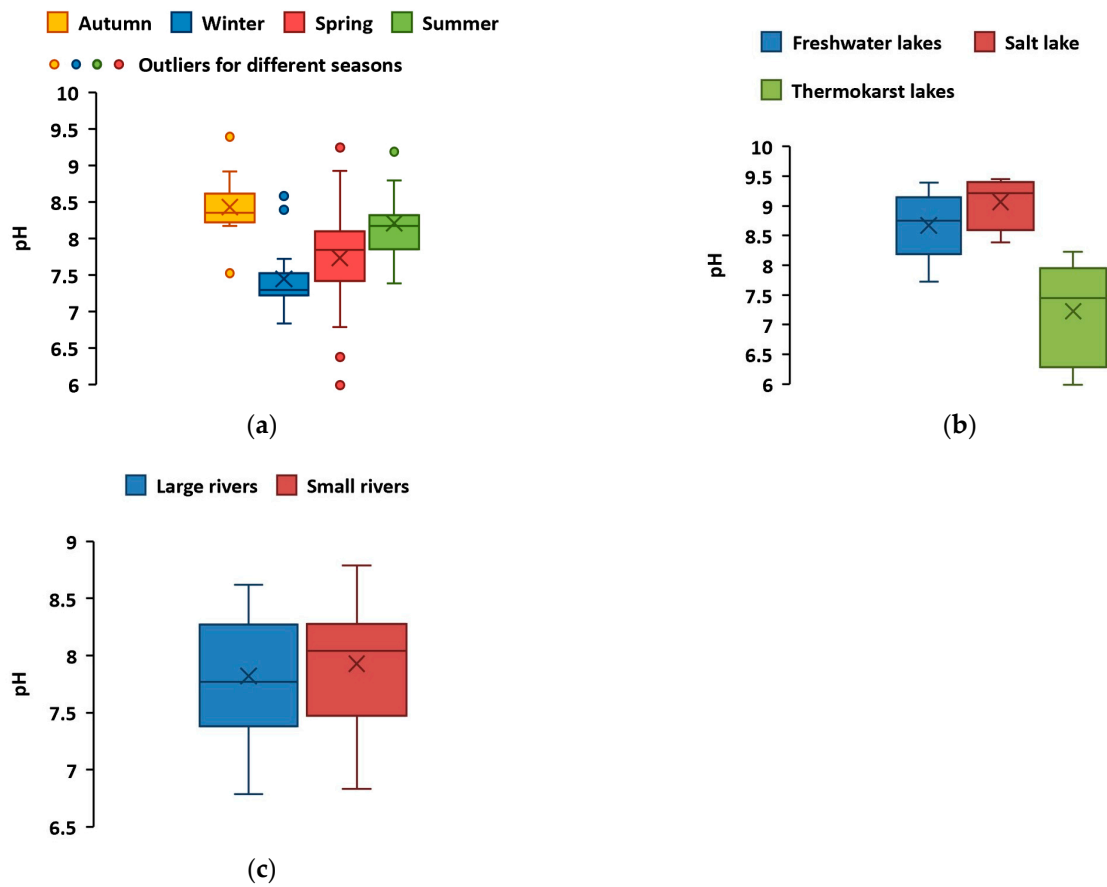


Figure 3. Boxplot of median pH values and IQR range (with outliers as dots) (a) during different seasons of the year (both rivers and lakes), and separately in (b) rivers and (c) lakes.

The water bodies of the Alash plateau, both rivers and lakes, exhibited the lowest E.C. In winter and autumn during low-water season, the electrical conductivity was significantly higher than in spring and summer ($F = 3.3, p = 0.03$), see Supplementary Figures S1 and S2. For lakes, a significant relationship ($p < 0.05$) between electrical conductivity and the pH was established (Figure 4). No such relationship was revealed for rivers. A strong direct relationship between electrical conductivity and DIC content was also observed (Figure 5), which reflected the dominance of bicarbonate ions in the major salt composition of both rivers and lakes (Supplementary Table S1).

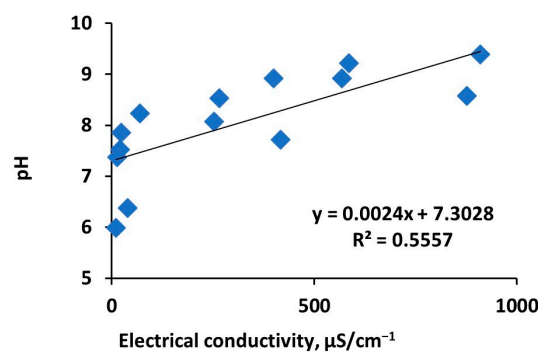


Figure 4. The relationship between electrical conductivity and DIC concentrations in the waters of the studied lakes (the salt lake Cheder is excluded).

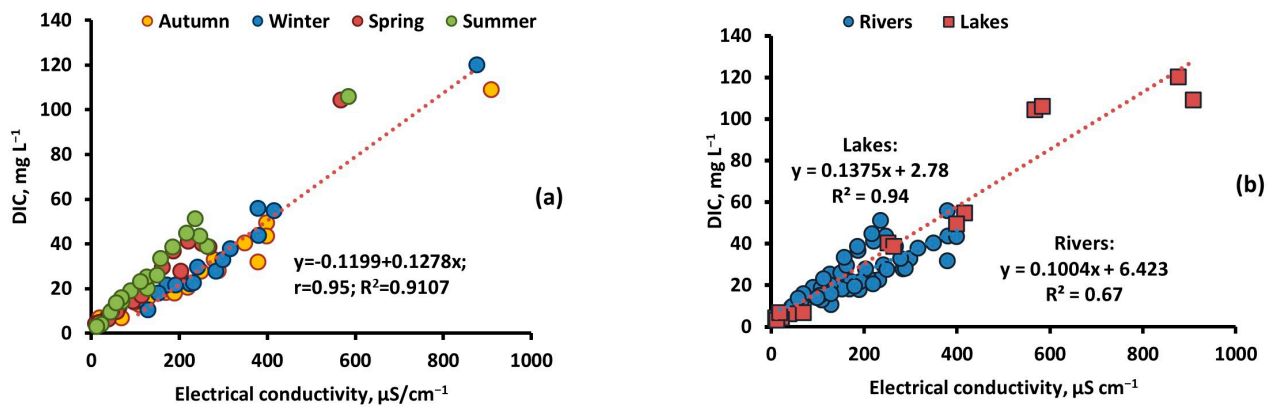


Figure 5. Linear relationship between DIC concentration and electrical conductivity in rivers and lakes of the Tyva region (a) in different seasons (lakes and rivers together) and (b) in different types of objects (averaged across seasons).

3.2. DIC vs. DOC Concentrations

Elevated DIC concentrations were observed in freshwater lakes, especially in Torehol Lake where they reached 120 mg L⁻¹, likely due to the impact of carbonate-rich groundwaters, which are reported to occur within the lake watershed (Figure 6a). The minimal DIC values were recorded in thermokarst lake waters, from 2.8 to 6.6 mg L⁻¹. The seasonal dynamics of DIC demonstrated rather low variations (within 30%) with minimal values observed in spring and maximal ones in winter, see Figure 6b.

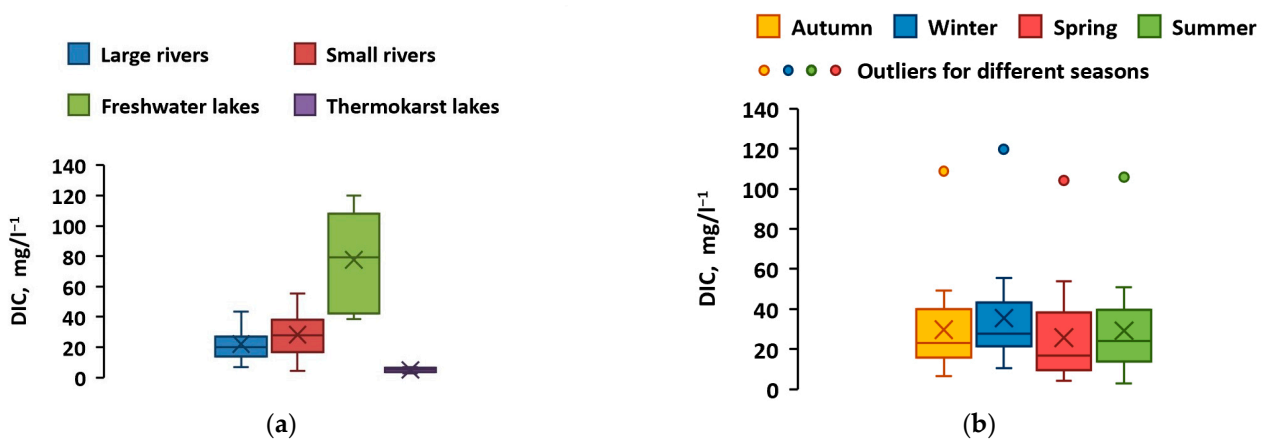


Figure 6. Median (and IQR) boxplots of DIC concentration (mg/L⁻¹) (a) in different types of objects (averaged across seasons) and (b) in different seasons (lakes and rivers together).

The maximal DOC values were measured in the waters of Torehol Lake and the thermokarst lakes. Of all the rivers studied, the Dyttyg-Khem, Durgen and Biche-Bayan-Kol waters were highly enriched in DOM, whereas the majority of the water bodies ranged from 2 to 6 mg L⁻¹ in DOC concentration. As in the case of DIC spatial and temporal patterns (Figure 6), the DOC concentrations demonstrated relative stability across seasons (Figure 7), with an exception of an anomalously high value (14.8 mg L⁻¹) in Torehol Lake during winter. The highest SUVA₂₅₄ values, which reflect the DOM aromaticity, were observed in the waters of thermokarst lakes, followed by rivers, whereas the minimal values were recorded in freshwater lakes (Figure 8a–c). The highest SUVA₂₅₄ was recorded in spring and the lowest in winter (Figure 8b).

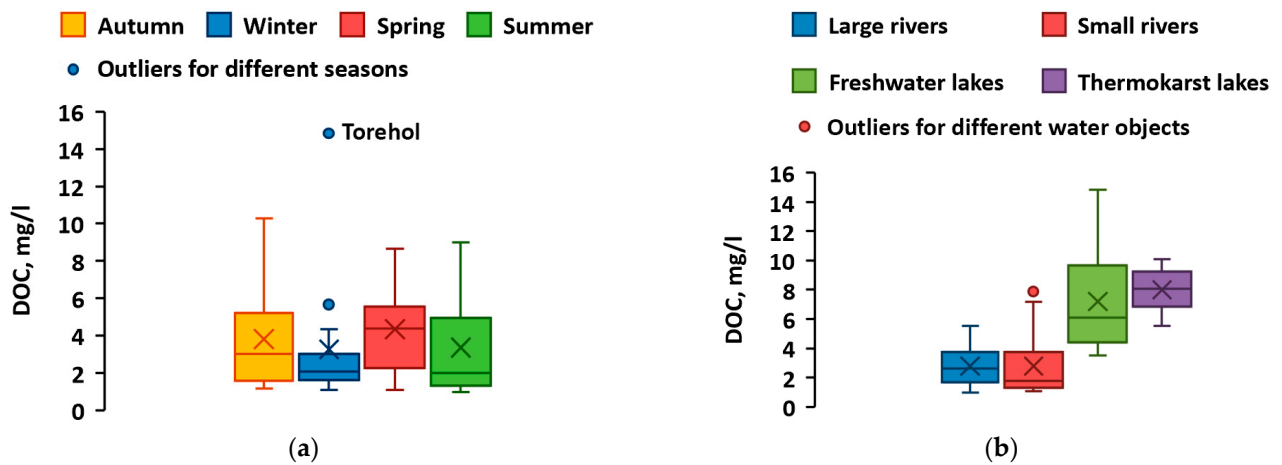


Figure 7. Median (and IQR) boxplots of DOC concentration (mg L^{-1}) in different types of objects (a) in different seasons (lakes and rivers together) and (b) in different types of objects (averaged across seasons).

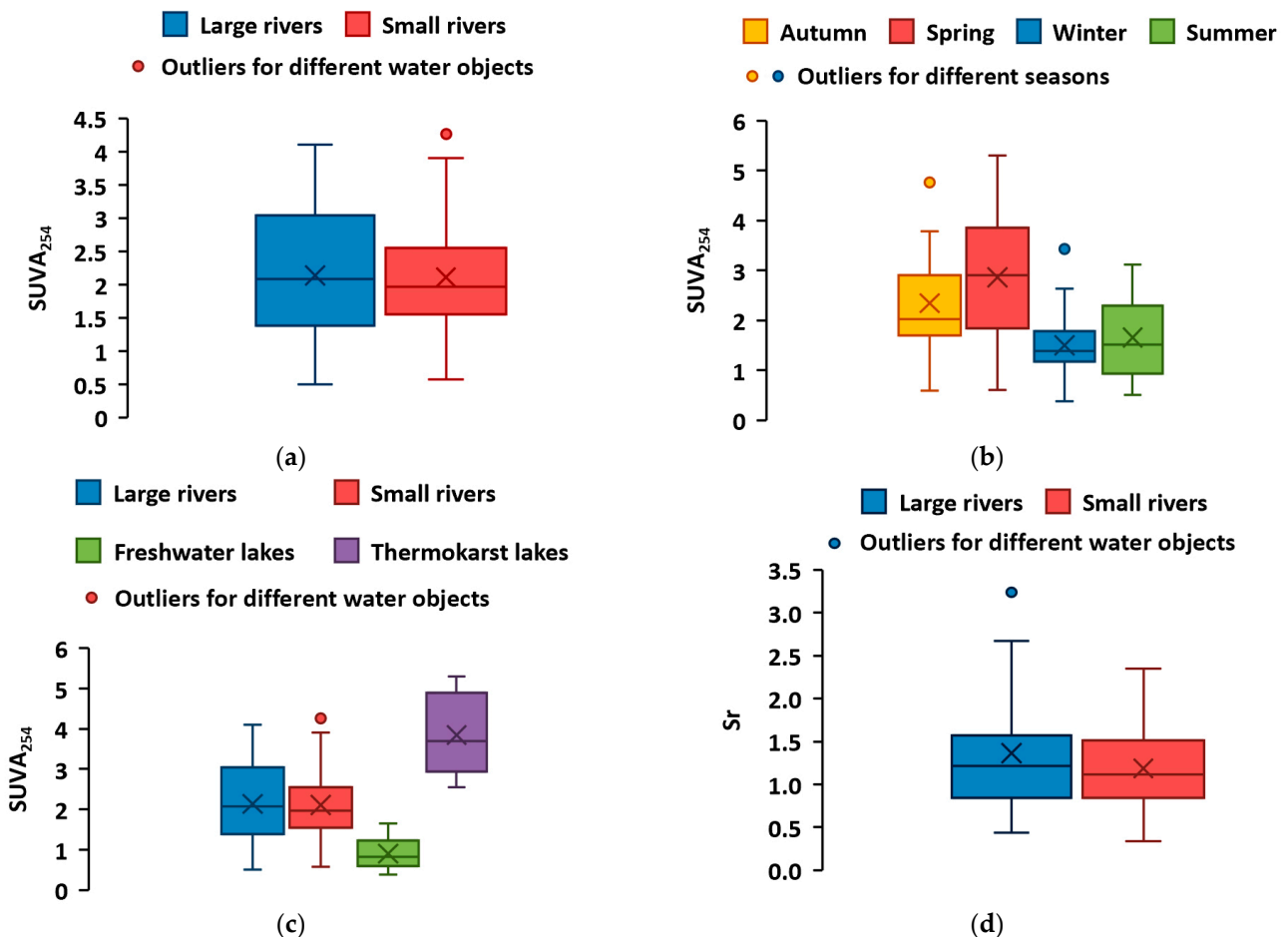


Figure 8. Median (and IQR) boxplots of SUVA₂₅₄ (a) in large and small rivers (averaged across seasons); (b) in different seasons (lakes and rivers together); (c) in different types of objects (averaged across seasons) and SR; and (d) in large and small rivers (averaged across seasons).

The ratio $E_{254}:E_{436}$ is known to indicate the relative role of allochthonous versus autochthonous organic substances in water bodies [76,77]. The DOM composition in the studied water objects was dominated by allochthonous substances, with the exception of the summer and part of the spring periods, when there was an increase in the $E_{254}:E_{436}$

ratio, indicating an active process of photosynthesis and destruction of detritus in the rivers and lakes themselves, leading to an increase in autochthonous organic matter [78,79].

There was no strong variation in the value of $SUVA_{254}$ in the waters of both small and large rivers (Figure 8a). However, small river waters had a lower S_R value, which indicated an increased degree of aromaticity compared to large rivers (Figure 8d). A high index of $SUVA_{254}$ ($3.8 \pm 1 \text{ L mg}^{-1} \text{ m}^{-1}$) and a low index of S_R (0.9 ± 0.1) in the waters of thermokarst lakes indicated the presence of high-molecular-weight aromatic compounds. In contrast, freshwater lakes, poor in DOC, exhibited much lower $SUVA_{254}$ and higher S_R values compared to thermokarst lakes. The ratio of optical densities $E_{254}:E_{436}$ in rivers followed the order 'summer > spring > autumn > winter' (Figure 9a). This ratio was much higher in thermokarst lakes compared to rivers and freshwater lakes (Figure 9b).

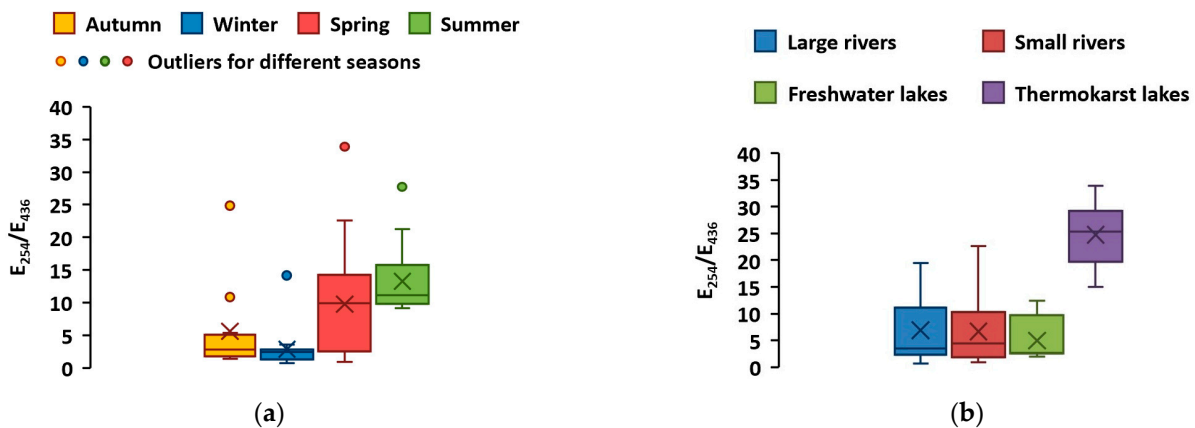


Figure 9. The ratio of optical densities E_{254}/E_{436} in the rivers and lakes of Tyva (a) during different seasons, and (b) for different types of objects, averaged across seasons.

3.3. Spatial and Seasonal Pattern of $p\text{CO}_2$ and $f\text{CO}_2$ in Rivers and Lakes

The highest values of $p\text{CO}_2$ were noted for a group of small rivers, with a maximum in the Adyr-Khem River, the smallest of the studied rivers draining the mound peat bog (Table 3). A high content of dissolved CO_2 was also noted in the waters of the Chadan River, originating in the western Tannu-Ola, and in the waters of the Khule River (Torgalyg), whose source is located on the eastern Tannu-Ola. This region (Tannu-Ola) is known for its CO_2 -rich underground discharges at the earth's surface. The average values of $p\text{CO}_2$ in large rivers differ significantly from small ones; the minimum was marked for the Alash River (Figure 10, Table 3).

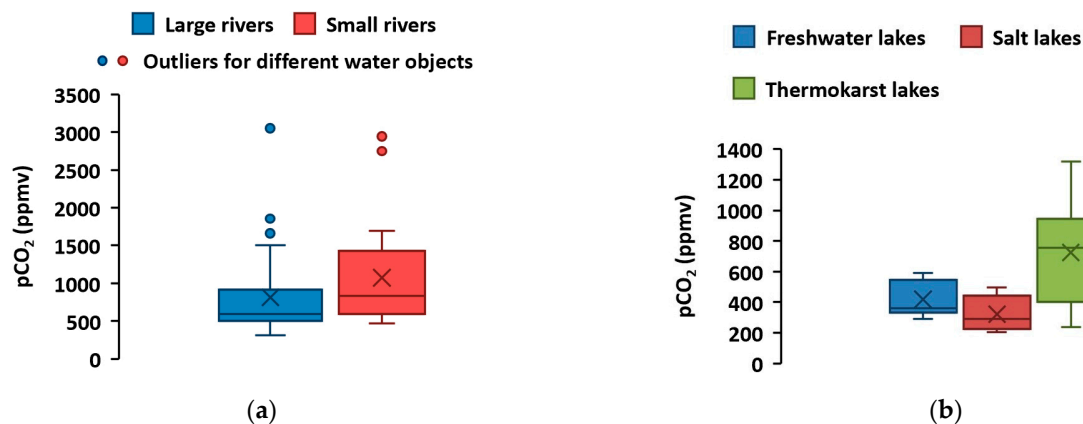


Figure 10. Median (and IQR) boxplots of CO_2 partial pressure (ppmv) in (a) rivers and (b) lakes, averaged across seasons. Different groups of rivers ($F = 5.42$, $p = 0.02$) and lakes ($F = 4.44$, $p = 0.03$) are significantly different.

Table 3. The values of pCO₂ (ppmv) in rivers and lakes of the region.

Rivers	Average	Median
Large rivers		
Yenisei	689	578
Big Yenisei	860	587
Small Yenisei	790	571
Tes-Khem	672	609
Khemchik	705	715
Alash	563	502
Small rivers		
Ak—Sug	809	552
Chadan	1470	1112
Durgen	739.5	493
Chaa-Hol	778	729
Huule (Torgalyg)	1133	1003
Anyyak-Chyrgaki	909	932
Dyttyg-Hem	840	660
Biche-Bayan-Kol	743	743
Adyr-Khem	2043	2105
Lakes		
Tore-Khol	332	337
Chagytai	504	535
Cheder	321	292
Thermokarst lake 1	754	705
Thermokarst lake 2	694	806

In lakes, the dissolved CO₂ content was sizably lower than that in rivers; the minimum values were noted for the salt lake Cheder and Tore-Khol Lake, located within a sandy substrate.

In terms of seasonal variations, in both rivers and lakes, the pCO₂ was significantly higher in winter due to CO₂ accumulation under ice (Figure 11). Note that because shallow thermokarst lakes freeze solid in winter, measurements of the water column during this period in these water bodies were not possible.

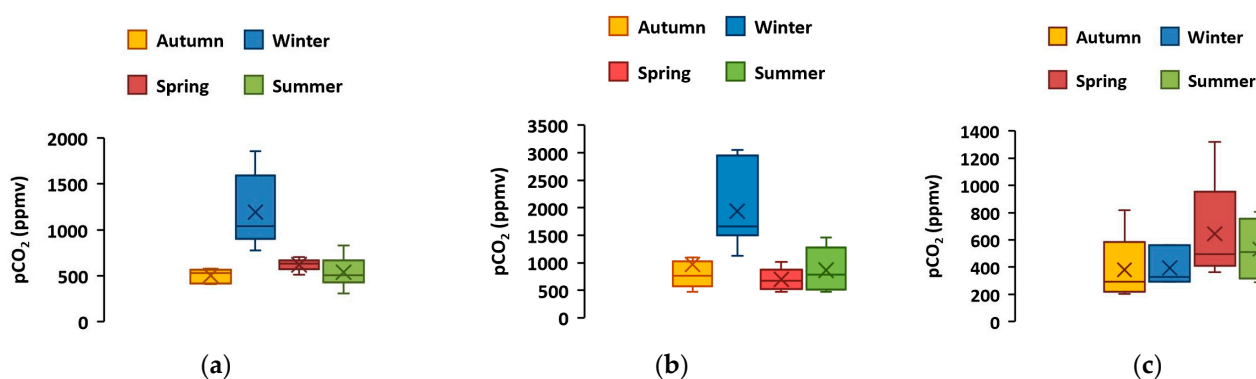


Figure 11. Median (and IQR) boxplots of CO₂ partial pressure (ppmv) in (a) large and (b) small rivers across seasons, which are statistically different (large rivers, $F = 12.20, p = 0.001$; small rivers, $F = 7.801, p = 0.001$, accordingly). (c) Median (and IQR) boxplots of CO₂ partial pressure (ppmv) in lakes across seasons ($F = 0.9223, p = 0.46$).

Overall, CO₂ emissions from the surface of rivers and lakes were quite low (median 0.05–0.15 g C m⁻² d⁻¹; Table 4) and did not differ significantly ($p > 0.05$) among water bodies, including the two main categories—rivers and lakes (Figure 12a,b). There was no

significant difference in fCO_2 between different seasons of the year (Figure 12c). Exceptionally high CO_2 fluxes in water were encountered in the Chadan River and the Ak-Sug River (12 and $5.6 \text{ g C m}^{-2} \text{ d}^{-1}$, respectively). Despite their small size, these rivers do not freeze solid during the ice-on period, and they likely possess sizable bicarbonate/ CO_2 -rich underground sources that are discharged at the river bed and hence are mostly pronounced during the winter baseflow.

Table 4. Measured fCO_2 fluxes ($\text{g C m}^{-2} \text{ d}^{-1}$) in rivers and lakes of the Tyva Republic (Sayan–Altai Mountain region).

	Autumn	Winter	Spring	Summer	Average Value	Median	Standard Deviation
Large rivers							
Yenisei	0.10	0.39	0.06	0.08	0.16	0.09	0.15
Big Yenisei		0.22	0.11	0.09	0.14	0.11	0.07
Small Yenisei	0.19	0.71	0.03	0.12	0.26	0.15	0.31
Tes-Khem	0.42	0.16	0.10	0.10	0.19	0.13	0.15
Khemchik	0.19	0.35	0.00	0.08	0.16	0.14	0.15
Alash	0.07	0.10	0.00	−0.02	0.04	0.03	0.06
Small rivers							
Ak—Sug	0.10	5.60	0.04	0.11	1.46	0.10	2.76
Chadan		12.11	0.01	0.13	4.08	0.13	6.95
Durgen	0.20	0.25	0.00	0.02	0.12	0.11	0.13
Chaa-Hol	0.31		0.04	0.15	0.17	0.15	0.14
Huule (Torgalyg)	0.14	0.15	0.05	0.45	0.20	0.15	0.17
Anyyak-Chyrgaki	1.89		0.06	0.33	0.76	0.33	0.99
Dyttyg-Hem		0.51	0.12	0.03	0.22	0.12	0.26
Biche-Bayan-Kol							
Adyr-Khem	3.58	0.48	0.16	−0.06	1.04	0.32	1.71
Lakes							
Tore-Khol	0.03	0.02	0.07	0.11	0.06	0.05	0.04
Chagytai	0.16	0.01	0.11	0.00	0.07	0.06	0.08
Cheder	0.07	0.09	0.05	−0.04	0.04	0.06	0.06
Thermokarst lake 1	0.09		0.06	0.04	0.06	0.06	0.02
Thermokarst lake 2	0.13		0.02	0.06	0.07	0.06	0.06

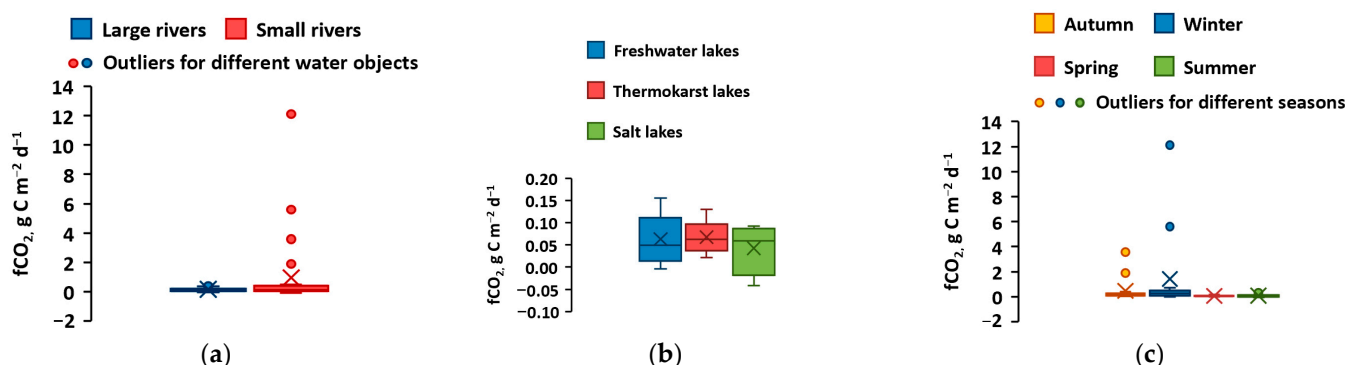


Figure 12. Boxplots (median and IQR range) of fCO_2 in (a) rivers, where the difference is insignificant ($F = 2.30, p = 0.13$); (b) lakes ($F = 0.30, p = 0.743$); and (c) all types of objects across seasons ($F = 2.54, p = 0.064$).

Analysis of correlations between O_2 and CO_2 concentrations of all objects across seasons did not allow us to establish any relationship ($r = -0.13, p > 0.05$); however, when

considering solely large rivers and thermokarst lakes, a negative relationship ($r = -0.47$ and $r = -0.95$) was observed (Table S1; Figure S4). In freshwater lakes, $p\text{CO}_2$ also negatively correlated with O_2 level ($r = -0.50$, $p < 0.05$). The water temperature exerted a significant ($r = 0.64$, $p < 0.05$) impact on $p\text{CO}_2$ in large rivers (Table S1).

3.4. Testing Potential Drivers of CO_2 Concentrations and Fluxes

During the summer period, the $p\text{CO}_2$ of the water column in lakes correlated with the lake water surface area ($p < 0.05$), whereas during other seasons, this relationship was not significant ($p > 0.05$); see Figure 13a. The flux of CO_2 positively correlated with lake surface area during the spring and winter periods ($p < 0.01$), as illustrated in Figure 13b. In thermokarst lakes, $p\text{CO}_2$ and $f\text{CO}_2$ increased with lake surface area in spring but decreased with S_{area} in summer and autumn (Figure S5), although these qualitative trends could not be statistically supported due to too low a number of sampled lakes. The river watershed area positively correlated with $p\text{CO}_2$ and $f\text{CO}_2$ ($p < 0.05$) in the autumn period, whereas during other seasons, the correlation was absent ($p > 0.05$), as shown in Figure S6.

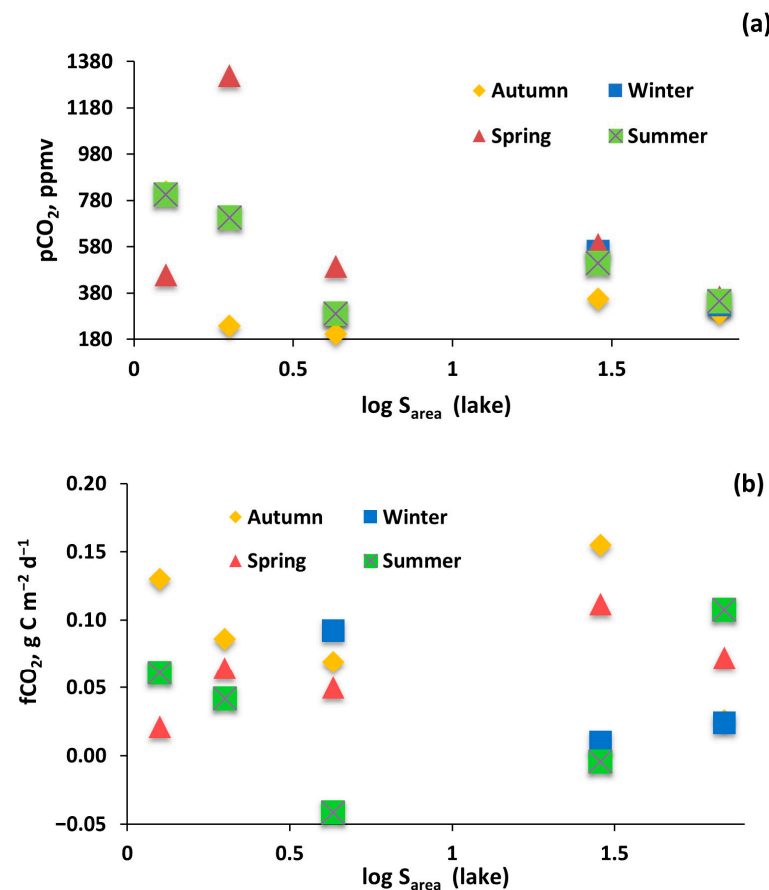


Figure 13. The relationship between (a) $p\text{CO}_2$ and (b) $f\text{CO}_2$ and lake water surface area of the Tyva region (all seasons together).

Among the ‘internal’ factors likely to control the CO_2 pattern (concentration and fluxes) in the water bodies, we tested major hydrochemical parameters of the water column, including pH, conductivity, DIC, DOC, concentration, DOM quality and a microbiological parameters (i.e., total bacterial count), as presented in Table 5. Considering all water objects together, neither $p\text{CO}_2$ nor $f\text{CO}_2$ correlated significantly ($r > 0.39$ at $p = 0.05$) with any tested parameter. Note that this result does not contradict several significant relationships of $p\text{CO}_2$ with lake area or O_2 , which were analyzed for individual seasons. Individual analyses of groups of rivers and lakes demonstrated strong positive control ($p < 0.05$) of

E.C. and pH on fCO₂ in large rivers ($r = 0.5$ and 0.64 , respectively) and negative control of pH on pCO₂ in lakes ($r = -0.99$); see Table S1 of the Supplement.

Table 5. Pearson correlation coefficients between major hydrochemical and microbiological parameters of the water column, including pH, O₂, S.C., DOC, DIC and optical parameters of DOM reflecting DOM quality. S_{area}, E.C. and TBC represent the area of the lake surface or the river watershed, electrical conductivity and total bacterial count, respectively.

All Objects													
All	E.C.	T _{water}	pH	O ₂	pCO ₂	TBC	DIC	DOC	SUVA ₂₅₄	E2:E3	E ₂₅₄ :E ₄₃₆	S _R	fCO ₂
S _{area}	0.03	0.16	0.23	0.23	-0.18	-0.29	-0.07	-0.46	-0.2	-0.05	-0.41	-0.14	-0.16
E.C.		0.05	0.76	0.25	-0.24	-0.01	0.95	0.23	-0.75	0.72	-0.48	0.85	-0.06
T _{water}			-0.26	-0.69	-0.12	0.02	0.19	0.11	0.01	-0.37	0.12	-0.11	-0.33
pH				0.54	-0.33	0.09	0.70	-0.01	-0.77	0.71	-0.58	0.61	-0.04
O ₂					-0.13	-0.16	0.06	-0.28	-0.42	0.53	-0.46	0.25	0.09
pCO ₂						0.00	-0.24	-0.28	0.29	-0.07	0.01	-0.15	0.85
TBC							0.14	0.33	0.09	-0.03	0.22	-0.16	0.05
DIC								0.26	-0.72	0.64	-0.44	0.75	-0.08
DOC									0.25	0.03	0.69	0.21	-0.23
SUVA ₂₅₄										-0.61	0.81	-0.56	0.08
E2:E3											-0.51	0.75	0.21
E ₂₅₄ :E ₄₃₆												-0.39	-0.16
S _R													0.06
Rivers													
	E.C.	T _{water}	pH	O ₂	pCO ₂	TBC	DIC	DOC	SUVA ₂₅₄	E2:E3	E ₂₅₄ :E ₄₃₆	S _R	fCO ₂
S _{area}	0.22	0.38	0.17	0.02	-0.46	-0.23	0.18	0.08	-0.06	-0.04	0.05	-0.06	-0.40
E.C.		-0.16	0.79	0.54	-0.05	-0.11	0.88	-0.21	-0.77	0.42	-0.53	0.34	-0.04
T _{water}			-0.37	-0.71	-0.19	0.16	0.06	0.11	0.18	-0.72	0.28	-0.46	-0.36
pH				0.67	-0.23	-0.18	0.65	-0.18	-0.78	0.61	-0.55	0.46	-0.09
O ₂					-0.07	-0.26	0.16	-0.16	-0.48	0.74	-0.44	0.66	0.06
pCO ₂						0.22	-0.05	-0.30	0.16	0.17	-0.20	0.17	0.93
TBC							0.02	0.32	0.17	-0.17	0.28	-0.40	0.12
DIC								-0.11	-0.68	0.14	-0.39	0.08	-0.08
DOC									0.45	-0.27	0.89	-0.54	-0.24
SUVA ₂₅₄										-0.36	0.75	-0.39	0.11
E2:E3											-0.49	0.65	0.33
E ₂₅₄ :E ₄₃₆												-0.58	-0.20
S _R													0.28
Lakes													
	E.C.	T _{water}	pH	O ₂	pCO ₂	TBC	DIC	DOC	SUVA ₂₅₄	E2:E3	E ₂₅₄ :E ₄₃₆	S _R	fCO ₂
S _{area}	0.95	0.58	0.72	0.11	-0.31	0.19	0.92	-0.32	-0.93	-0.53	-0.83	0.98	0.17
E.C.		0.56	0.75	0.17	-0.38	0.41	0.99	-0.15	-0.87	-0.25	-0.77	0.92	0.07
T _{water}			-0.07	-0.51	0.19	-0.38	0.57	-0.29	-0.45	-0.14	-0.41	0.46	-0.53
pH				0.59	-0.54	0.65	0.71	0.16	-0.68	-0.28	-0.53	0.75	0.55
O ₂					-0.92	0.54	0.14	0.20	-0.35	-0.03	-0.30	0.18	0.16
pCO ₂						-0.46	-0.35	0.05	0.59	0.08	0.57	-0.36	0.10
TBC							0.45	0.34	-0.19	0.39	-0.16	0.26	0.36
DIC								-0.17	-0.84	-0.19	-0.76	0.90	0.05
DOC									0.48	0.68	0.67	-0.42	0.02
SUVA ₂₅₄										0.58	0.96	-0.94	-0.06
E2:E3											0.59	-0.59	-0.42
E ₂₅₄ :E ₄₃₆												-0.89	-0.02
S _R													0.28

We found that TBC does not correlate with any parameter of the CO₂ system in rivers except in weak positive correlations with DOC ($R_{\text{Pearson}} = 0.32$, $p > 0.05$). In lakes, there were weak but not significant ($p > 0.05$) correlations with DOC ($R_{\text{Pearson}} = 0.31$) and fCO₂ ($R_{\text{Pearson}} = 0.36$, Table 5). This mostly occurred in thermokarst lakes (Table S1). It is therefore possible that some bacterial processing of DOC in the water column (biodegradation) generates excessive CO₂ emissions. However, these processes are obscured by other external factors of CO₂ delivery to the river or lake, which occur throughout soil and surface waters, respiration of sediments or biodegradation of particulate organic matter.

It is also important to note that wind speed might strongly affect the CO₂ emission fluxes, especially in wind-unprotected large lakes. Unfortunately, because we did not use wind-speed-based flux calculations [75] in this study, some environmental controllers listed in Table 5 could have exhibited a lower impact on fCO₂ than it occurs under field conditions.

4. Discussion

4.1. Major Solutes, Dissolved Organic and Inorganic Carbon

It is known that inland water systems are sizable sources of CO₂, which is a highly important prerequisite for the retroactive link between the climate and C cycle in aquatic systems [80–82]. Although at present, the climate changes in the territory of Tyva are already strongly pronounced (e.g., ref. [83]), it is not yet possible to quantify this impact on water bodies. However, the present study can provide a solid background for assessing the current status of C cycle in order to be able to judge the future changes which are likely to occur over the next decades.

The level of DIC concentration was sizably higher than that of DOC, and hence the C export in the studied rivers and C storage in the lakes are dominated by inorganic carbon. Only during spring was the DOC concentration higher than DIC, which could be linked to the snow melt, dilution of the groundwater signal and the dominance of surface flow. In particular, enhanced DOC delivery to lakes and rivers occurs during melt-snow interaction with surface soil and organic-rich litter. This period contrasts with the shallow subsurface flow in summer and autumn, when the water hydrochemical signal is essentially controlled by rock weathering at the watershed. In this regard, the present study corroborates the knowledge of processes controlling river and lake water chemical composition across seasons as established in the boreal, high latitude and subarctic rivers [84–86] and subarctic lakes [87]. Note here that the connection between the groundwaters and the lake, especially in permafrost-covered regions such the Altai–Sayan Mountain system, is weaker than that for rivers. A comobilization of DIC and other ions from shallow subsurface/groundwaters, bearing the signal of chemical weathering, for all water objects is confirmed by the observation that the DIC values strongly correlated with the electrical conductivity index. In the Khemchik, Ak-Sug, Alash and Adyr-Khem mountain rivers flowing in the northwestern part of the Republic of Tyva in the Western Sayans, the DIC concentration ranged from 4 to 20 mg L⁻¹ and in other rivers from 9–13 to 55 mg L⁻¹. It is possible that a reason for such reduced DIC values in mountain rivers is an increased precipitation in this area [83], the presence of permafrost [88] and high runoff [89]. An opposite situation is observed in the water bodies of the more arid Ubsu-Nur basin: Tore-Khol Lake and the Tes-Khem River, where the DIC values are the highest. Here, evaporative concentration of major solutes, occurring both within the river watersheds and the lake water column, can be responsible for elevated DIC and S.C. values.

Increased DOC concentrations were observed in lakes compared to rivers, which may be explained by higher water residence time and autochthonous production of OM. This was especially pronounced in thermokarst lakes, which exhibited the highest SUVA (Figure 8b,c) and humification index (E₂₅₄/E₄₃₆ ratio) (Figure 9b). The delivery of allochthonous material to the water bodies occurs essentially during summer and spring following the shallow water paths through organic-rich soil layers (Figure 9a). According to the ratio of optical densities E₂₅₄/E₄₃₆, allochthonous (peat-originated) organic matter prevails in thermokarst lakes and significantly exceeds the values of the ratios in other water bodies. Low water residence time in thermokarst lakes, their small size and their location within wetland zones may lead to sizable accumulation of terrestrial humic-rich organic matter. Much lower values of the optical index E₂₅₄/E₄₃₆ in rivers and freshwater lakes likely correspond to a decrease in the humification index [90] due to biotically driven degradation of humiclike aromatic components in these water objects with high water residence time [91].

4.2. Dissolved C Pattern and CO₂ Fluxes: Driving Factors and Comparison with Other Regions

We identified the oxygen regime as one of the main controlling factors of pCO₂ level in both rivers and lakes across seasons. The highest CO₂ concentrations were observed in O₂-impoverished waters, likely due to the important impact of partially anoxic sediment respiration on the CO₂ regime of the water column. Similar effects are reported in many boreal and subarctic waters across the world, notably in lakes and channels of the Ob River floodplain (e.g., ref. [73]).

The $p\text{CO}_2$ was generally higher in lakes of a smaller surface area, which is a well-known phenomenon in various lakes of the boreal and subarctic zones [1,75]. This can be linked to enhanced terrestrial input of CO_2 -rich waters from the watershed in small lakes and sizable primary productivity of plankton and periphyton/macrophytes in large, mature lakes, leading to CO_2 uptake in the latter, as it is known in thermokarst water bodies in the neighboring territory of permafrost peatlands [92].

The seasonal variations of CO_2 concentration were characterized by a maximum $p\text{CO}_2$ during winter in rivers and during spring in lakes. The former can be explained by enhanced underground discharge within the river's main stem and CO_2 accumulation under ice, whereas the spring maximum of CO_2 in lakes is likely due to a lack of phytoplankton activity and the enhanced input of biologically labile terrestrial DOM from the watershed during freshet. This DOM can be subjected to intensive bacterial processing leading to a maximum of CO_2 emissions [93]. In the summer period, lakes act as a CO_2 sink due to biological production processes (macrophytes, cyanobacterial bloom) in the water column (e.g., ref. [94]).

The data on carbon (DOC, DIC, CO_2) concentrations and CO_2 fluxes in the Altai–Sayan mountain system were compared with the data reported for the Qinghai–Tibetan–Plateau [18,95,96], since this region has relatively similar climate and is also impacted by permafrost. To account for thermokarst lakes, we chose the largest compilation of lakes in the sporadic to continuous permafrost zone of Western Siberia, reported in Serikova et al. (2019) [1]. A synthesis of available information is provided in Table 6. The DOC levels of rivers and lakes of the Tuva Republic obtained in this study are quite similar within the range of natural seasonal and spatial variations to those in thermokarst lakes of the QTP as well as the Tibetan rivers. The DIC concentrations in lakes and rivers of the Sayan–Altai Mountain system are also similar to the values of the Qinghai–Tibetan plateau, with the exception of saline lakes, whose C cycle is strongly controlled by local evaporative processes.

Table 6. Comparison of carbon concentrations in lakes and rivers and CO_2 (mean and standard deviation) emissions from water surfaces in the Tyva region to other regions of the world that have similar climate and landscape parameters.

Sites	Period	$p\text{CO}_2$ (ppmv)	$f\text{CO}_2$ ($\text{g C m}^{-2} \text{d}^{-1}$)	DOC (mg L^{-1})	DIC (mg L^{-1})	Reference
All	Annual cycle	1495 ± 577	0.46 ± 1.6	3.7 ± 2.9	29 ± 24	This study
Rivers	Annual cycle	929 ± 611	0.60 ± 1.9	2.7 ± 1.7	24.6 ± 12	This study
Lakes	Annual cycle	385 ± 123	0.06 ± 0.05	7.2 ± 3.8	78 ± 35	This study
Thermokarst lakes	Annual cycle	724 ± 368	0.067 ± 0.038	8 ± 1.6	5 ± 1.6	This study
Fenghuoshan catchment, China	Annual cycle	1260 ± 145	6.3 ± 0.9	17.9 ± 5.5	33 ± 3	[19]
Thermokarst lakes, China	June–September			9.5 ± 5.7	38 ± 35	[96]
The NamCo basin and source area of Yellow River (SAID)	July 2015 (melting of glacier)			2.3 ± 1.3	11.3 ± 10.6	[97]
Yangtze River source region	Biweekly from May to October	1086 ± 275		2.8 ± 0.6	24.4 ± 1.9	[18]
Qinghai Lake and the inflowing rivers	23 May 2021			1.0 ± 0.6	13.3 ± 7.7	[21]
Three catchments within the Nam Co watershed	June/July 2018, May 2019 and September 2019			2.4 ± 0.3	8.8 ± 5.5	[98]
76 lakes, Western Siberia Lowland	May–June, August–October	1044 ± 1540	1.7 ± 1.7	16 ± 10	0.7 ± 0.8	[1]
Lena upstream of Kirenga	29 May to 17 June 2016	714 ± 22	0.85 ± 0.06	13.9 ± 1.4	20.0 ± 1.2	[74]
Southwestern and northeastern regions of the QTP (70 lakes, four rivers and one reservoir on the QTP)	20-year period (i.e., from the 2000s to the 2020s)		0.3 ± 0.2			[95]
Two saline lakes (Qinghai Lake and Hala Lake) in the Tibetan Plateau	Continuously measured on 20, 23 October 2018		13.1 ± 0.4			[20]

In contrast to the DIC and DOC concentrations, for which the results of different regions are fairly comparable, the $p\text{CO}_2$ in the Sayan–Altai Mountain region had generally lower values than those observed in the Qinghai–Tibetan Plateau and Western Siberia. It is possible that sizable autochthonous production and CO_2 uptake by plankton in lakes and by macrophytes in rivers could be partially responsible for lower CO_2 levels in the water bodies of the studied region during the summer period, when the water temperature becomes higher than that in subarctic Western Siberia or high-altitude QTP. At the same time, our results on CO_2 flux are comparable to those of Jia et al. (2022) [95] for the lakes and rivers of southwestern and northeastern regions of the QTP ($0.3 \pm 0.2 \text{ g C m}^{-2} \text{ d}^{-1}$). However, unlike the maximal flux observed in the present work during winter, the latter authors reported the lowest flux during ice-covered seasons. The lowest CO_2 emission is typically observed during cold periods, as also reported by other studies [96–100]. In our case, high wintertime $p\text{CO}_2$ and $f\text{CO}_2$ could indicate the existence of sizable underground sources of CO_2 (discharge of CO_2 -rich fluids, especially pronounced during low-water-level periods). These effects are visible for large rivers, which demonstrated strong positive impact of E.C., pH and DIC on $f\text{CO}_2$ (Table S1).

Overall, the differences of CO_2 emissions among different works on northern and mountain aquatic systems may be due to the peculiarities inherent to our region as well as differences in the methodologies used. It is interesting that the carbon uptake flux in the terrestrial Tyva steppe regions is estimated as $184 \pm 41 \text{ g C m}^{-2} \text{ yr}^{-1}$ [101]. This is fairly comparable with the CO_2 emission flux from the rivers of the region, assessed in the present study ($213 \text{ g C m}^{-2} \text{ yr}^{-1}$). Such a comparison is consistent with the importance of inland water bodies (rivers and lakes) in overall C balance of the terrestrial biomes, as also demonstrated in Western Siberia [102]. However, at the present status of the research, a straightforward comparison of the data on the C pattern revealed in the Sayan–Altai region and those reported in the adjacent subarctic and mountain territories requires more thorough assessment of possible controlling factors such as local climate variation, productivity of the terrestrial compartments, underground influx, respiration of sediments and primary productivity in the river and lakes. In particular, it was beyond the scope of the present study to address the soil type and chemical weathering within each individual catchment of a river or lake. Future research will focus on relating the GIS-based specific watershed parameters (including soils, vegetation, climate and lithology) and CO_2 emissions pattern, as it was recently developed for a number of rivers in Siberia (e.g., refs. [2,72,74]).

5. Conclusions

A thorough, first-time assessment of the contemporary status of the C biogeochemical cycle (concentration in and emission from the water surfaces) was conducted in lakes and rivers of the Central Asian Sayan–Altai Mountain system in order to provide a background for judging possible future changes induced by particulate climate instability in this region. Using a physicogeographical and climatic transect of inland water bodies, which comprised a large variety of natural ecosystems and landscapes of the region, we found that permafrost exerts the largest impact on lake water hydrochemistry and C pattern including CO_2 exchange with the atmosphere, whereas the size of the river watershed had relatively little impact on the CO_2 pattern. In contrast, $p\text{CO}_2$ decreased with an increase in lake size, which could be linked to a combination of factors, notably (i) enhanced input of terrestrial, biolabile DOM in small lakes which served as a source of CO_2 production in the water column; (ii) terrestrial input of CO_2 -rich shallow groundwater and soil waters, more pronounced in small lakes; and (iii) CO_2 uptake in large lakes due to macrophytes, periphyton and phytoplankton activity. The oxygen regime was found to be an important controlling factor of the $p\text{CO}_2$ level in both rivers and lakes during specific seasons, likely due to sediment respiration processes. However, despite these qualitative features of possible CO_2 regime control in the studied water bodies, a pairwise correlation analysis did not demonstrate statistically significant relationships between CO_2 flux and physicogeographical parameters of river watersheds, river and lake size and internal parameters of the water

column, including basic hydrochemical characteristics, DOM concentration and quality and bacterial concentration. A likely reason is the complexity of the ‘external’ and ‘internal’ factors controlling the CO₂ exchange between water surfaces and the atmosphere and their frequent counteraction of CO₂ production/uptake in the water column, sediments and the watershed.

We argue that further assessment of possible controlling factors such as local climate variation, productivity of the terrestrial compartments, underground influx, respiration of sediments and primary productivity in the rivers and lakes are necessary for comparison of the aquatic C pattern revealed in the Sayan–Altai region in this study to those reported in the adjacent subarctic and mountain territories.

Supplementary Materials: The following supporting information can be downloaded at: <https://www.mdpi.com/article/10.3390/w15193411/s1>, Figure S1. Box plot of median and IQR range (with outliers as dots) of electrical conductivity in rivers (a); lakes (b); DIC concentrations in rivers (c); and lakes (d), averaged across seasons. Figure S2. Boxplots (median and IQR range) of electrical conductivity during different seasons (lakes and rivers combined together). Figure S3. Plots of DIC concentration (mg L⁻¹) as a function of electrical conductivity in large rivers (a), small rivers (b) and lakes (c). Figure S4. The relationship between pCO₂ and oxygen saturation degree of lake and river waters in the Tyva region (all seasons together). Figure S5. The relationship between (a) pCO₂ and (b) fCO₂ and thermokarst lakes water surface area of the Tyva region. Figure S6. The relationship between pCO₂ (a) and fCO₂ (b) in river watershed area in the Tyva region (all seasons together). Table S1. Pearson correlation coefficients between major hydrochemical and microbiological parameters of the water column, including pH, O₂, S.C., DOC, DIC and optical parameters of DOM reflecting DOM quality. S_{area}, S.C., and TBC represent area of the lake surface or river watershed, Electrical Conductivity, and Total Bacterial Count, respectively.

Author Contributions: Conceptualization, A.A.B., L.G.K., A.O.K. and S.K.; methodology, I.I.K., T.V.R., A.S.P., I.V.L., Z.N.K. and S.N.V.; software, I.I.K.; validation, S.N.V. and O.S.P.; formal analysis, A.A.B. and L.G.K.; investigation, A.A.B., L.G.K. and I.I.K.; resources, A.O.K. and S.K.; data curation, A.A.B. and L.G.K.; writing—original draft preparation, A.A.B. and L.G.K.; writing—review and editing, O.S.P.; visualization, A.A.B. and L.G.K.; supervision, S.K.; project administration, A.O.K.; funding acquisition, S.K. and A.O.K. All authors have read and agreed to the published version of the manuscript.

Funding: This research was funded by Tomsk State University Development Program “Priority 2030” (A.A.B., L.G.K., I.I.K., T.V.R., A.S.P., S.N.V., O.S.P., S.K.) and grant RSCF № 23-14-20015 (A.O.K). Research was performed using the equipment of the unique research installation ‘System of experimental bases located along the latitudinal gradient’ with financial support Ministry of Science and Higher Education of Russia (RF-2296.61321X0043, 13.UNU.21.0005, contract No. 075-15-2021-672).

Data Availability Statement: Full data set of this study is available at the Mendeley Data Portal: Byzaakaу, Arisia; Лариса, Колесниченко; Pokrovsky, Oleg (2023), “Dissolved carbon concentrations and emission fluxes in rivers and lakes of Central Asia (Sayan–Altai mountain region, Tyva)”, Mendeley Data, V1, <https://data.mendeley.com/datasets/d35ctw7tb3/1>, accessed 23 September 2023.

Conflicts of Interest: The authors declare no conflict of interest.

Appendix A

Detailed description of rivers and lakes of the Tyva Republic sampled in this work.

The Yenisei River is one of the longest and deepest rivers in the world and Russia, flowing into the Kara Sea of the Arctic Ocean. The length is 3487 km, the catchment area is 2,580,000 km², and the annual flow is 624.41 km³. The flow velocity is from 0.3 to 5 m/s, depending on the location of the river [103]. The research was carried out in the upper reaches of the river. The river originates from the confluence of two sources—the Big Yenisei (Biy-Khem) and the Small Yenisei (Kaa-Khem). The main tributaries in the upper reaches are Elegest, Khemchik, Us, Kantegir. The city of Kyzyl and the Service-Khem kozhuun of the Republic of Tyva, together with the administrative center of Shagonar, is located in the river basin. The non-flooded channel of the Upper Yenisei (Service-Khema)

on the territory of Tyva runs through the flat terrain of the Tuva basin with a pronounced steppe landscape, has many channels and islands [104].

The basin of the Bolshoy Yenisei River (Biy-Khem) is located in the wettest, taiga, teeming with lakes and wetlands of Tyva. In the center of it is the vast Todzhinsky basin. The Biy-Khem basin, in the area from the mouth of the Seiba to the mouth of the Uyuk, is characterized by the presence of high mountains with steep slopes and weak forest cover. Below, before the confluence with the Maly Yenisei River (Kaa-Khem), smoothed open landforms and a wide river valley are typical. The length of the river is about 560 km. The width of the riverbed The Yenisei varies from 20–80 m in the upper reaches to 120–290 m in the middle and lower reaches, depths, respectively, from 1–1.5 m to 1.5–4 m. The flow velocity varies from 1.4 to 2.4 m/s. The average long-term water consumption of the Yenisei River in the closing alignment (Kara—Haak village) is 594 m³/s [104].

The Maly Yenisei River (Kaa-Khem) is formed by the confluence of two rivers: Kyzyl-Khem and Balyktyg-Khem. The source of Kyzyl-Khem is located on the territory of Mongolia, whereas Balyktyg-Khem originates from the northern slopes of the Sengilen Highlands. In the upper reaches of the Yenisei River, it is a typical mountain river, its bed abounds with rocky ledges that form numerous rapids and shivers. After entering the Ulugh-Khem basin, it flows in low steppe shores. Compared to Biy-Khem, Kaa-Khem has fewer tributaries. The right tributaries of the river are Unzhey, Honga, Uzhep, Derzyg; the left ones are Shivey, Sizim, Buren. The river is quite full-flowing, fast, the speed is 1.8–2.3 m/s, the width of the channel is from 20 to 80 m. The water discharge is highly variable and depends on the amount of precipitation (Table 1). In May–early June, the spring flood comes, and in July–August, as a result of heavy rains, sometimes there is a summer flood. Groundwater takes part in feeding rivers all year round. The depth of groundwater is about 8–10 m, in floodplains of rivers and streams they come close to the surface [105].

The Tes-Khem River has a mountainous character, belongs to the Ubsu-Nur water system. The length of the river is 139 km, the width of the river is 10–100 m, the catchment area is 4390 km². The river's feeding is predominated by rain. In summer, there is a high probability of rain floods. In winter, the river freezes. The river originates on the Tannu-Ola mountain range. The mouth of the river is at an altitude of 1067 m. To the west of Tes-Khem, beyond the sands of Tsugeer-Els, there is the lake Tore-Khol, formed by the damming of the former tributary of Tes-Khem.

The Khemchik River originates on the eastern slope of the Kozer ridge from a peak of 3122 m, belonging to the Shapshalsky ridge system, on the border with the Altai Republic. The entire river is located on the territory of the Republic of Tyva. It flows between two mountain systems—the Western Sayan from the north and the Western Tannu-Ola from the south, collecting all its runoff from them. The length of the river is 320 km, the catchment area is 27 thousand km². The average water discharge is 102 m³/s [104]. All sources and tributaries are fed by runoff from high ridges, and therefore the river system in the Khemchik basin is widely used for irrigation [106]. The valley is narrow, with steep banks, and there are many boulders in the riverbed. In the Khemchik basin, the river has a flat character with bends. Large stone remains are not uncommon. The flow velocity is low. The river is essentially fed from underground discharge. The Khemchik's flood occurs in summer, from June to August inclusive (with a maximum in July), and is the result of summer precipitation in the form of rain. In September, water consumption decreases significantly, and this decrease continues until the beginning of winter, along with a decrease in precipitation [107].

The Alash River, a left tributary of the Khemchik River, is formed by the confluence of the Chulcha and Kara-Khol rivers; its length is 125 km and the slope is up to 3.5 m/km. The catchment area is 4630 km. The width of the riverbed is up to 60–90 m. The valley of the river is wide. The river acquires a mountain-steppe character. Absolute elevation marks in the area of the river flow range from 1000 to 1200 m [108].

The Ak-Sug River (in the upper reaches of the Ak-Khem), a left tributary of the Khemchik River, originates in one of the lakes of the Dashtyg-Khem ridge at an altitude of 2115 m above sea level. The length of the river is 160 km, the area of its catchment area is 3170 km². The average annual water discharge is 14 m³/s. Agriculture with irrigation is developed in the valley. Annual water consumption is 1% of the annual flow of the river (15 million m³). The river has 46 tributaries less than 10 km, the total length of which is 173 km, there are also 82 lakes in the catchment area, the total area of which is 10.23 km². The Kyzyl-Taiga Mountain is located at the headwaters of the Ak-Sug River [109]. The absolute heights of the terrain through which the Ak-Sug River flows vary significantly from 1320 to 2100 m. The width of the riverbed ranges from 2–5 m in winter, to 15–20 m in summer, the depth, respectively, from 0.2–0.3 m to 0.7–1.1 m. The river valley on the investigated section of the Ak-Sug river is forested, the lower parts of the slopes are relatively flat, the upper ones with rocky and shrubby tundra are steep and rocky. At the beginning of the lower third of this segment on the left bank of the Ak-Suga at absolute altitudes of 1350–1500 m there is an eponymous deposit of molybdenum-copper sulfide ores. The deposit was exposed by erosion and subjected to the movement of part of the ore material by a glacier [110].

The Chadan River is a right tributary of the Khemchik River. The source is located on the western ridge of Tannu-Ola. The length of the watercourse is 98 km, the catchment area is 2200 km². The absolute height of the terrain is 800 m [111].

The Durgen River is a left tributary of the The Yenisei of the 3rd order: flows into the Mezhegey River, a tributary of the Elegest River. The source is located in the highlands of the East Tannu-Ola ridge, then the river flows along its northern macro slope. According to the State Water Register, the total length of the river is 93 km. The speed of the river flow changes in accordance with the change in terrain. The river is distinguished by a rare cascade of waterfalls. The river is located within the Mezhegeysky coal deposit (Khayan et al., 2014) [112]. In the middle course, the river flows through the territory of two villages in which there is no sewerage, the river is used for watering livestock. Part of the catchment area is occupied by a specially protected natural area—the Durgensky Nature Reserve.

The Chaa-Khol River, a right tributary of the The Yenisei River, flows through the territory of the Ulug-Khem and Chaa-Khol kozhuuns of Tyva. The total length of the river is 90 km. The catchment area has 1730 km². It begins on the northern slope of the Western Tannu-Ola ridge between the Tyndy-Ula and Hule-Bozh mountains. It flows in a northerly direction through a valley overgrown with larch forest in the upper reaches and across the steppe in the lower reaches. In the middle course it is divided into several channels. It flows into the Yenisei River at a distance of 3315 km from the mouth. The height of the mouth is 540 m above sea level [103].

The Khule River (Torgalyg), a right tributary of the Shagonar River, originates on the northern macroscline of the Eastern Tannu-Ola, flows through the Central Tuva Basin. The length of the river is 40 km, the width varies from 0.5 to 1.5 m, the catchment area is 610 km². Altitude above sea level: 535 m [113].

Anyyak-Chyrgaki River, a tributary of the Chirgaki River, a right tributary of the Khemchik River. The length of the watercourse is 52 km, the catchment area is 410 km². The bottom of the river is pebbly. During the study period, the water is transparent to the bottom, its color is bluish-green, the depth of the river ranges from 0.2 to 2.0 m. The absolute elevation of the terrain is 800 m. The source of the river begins on the north-western forested slopes of the Western Tannu-Ola [114].

The Biche-Bayan-Gol River is a right tributary of the Yenisei, into which it flows 12.5 km from the mouth, 14 km northwest of the city of Kyzyl. The length of the watercourse is 32 km [115].

The Adyr-Khem River flows through the territory of the Barun-Khemchik district on the Alash plateau. The width of the Adyr-Khem River is 1.5 m, the depth is from 0.25–1 m, the flow velocity is about 0.25 m/s [116].

Lake Tore-Khol is the only large freshwater lake in the Ubsunur basin. The lake has no tributaries, receiving water from springs of sand dunes, which are located in a horseshoe-shaped bowl of the southern shore and drain into the lake in the form of a stream. The Torehole is located in a shallow depression with flat sides, the average depth is 7 m, the area is 42 km². The greatest depth (up to 40 m) was noted at the isthmus in the southern part. The absolute height of the terrain is 1149 m. The lake is oligotrophic, the least productive of all the lakes of the Ubsunur basin [117]. It contains a relatively small percentage of organogens and bacteria. Therefore, the lake is transparent, clean, rich in underutilized oxygen by organisms. In the summer, the surface layers warm up well, in the middle of August in the afternoon the temperature rises to 21 °C at an air temperature of 32 °C [118].

Lake Chagytai is the largest freshwater lake of the Tuva basin, located in its southern part on the border of the settled hilly foothills of the Vostochny Tannu-Ola ridge, at an altitude of 1003 meters above sea level. This is the largest freshwater lake in the Tuva basin. It has the shape of an almost regular circle with a diameter of about 6 km, the length of the coastline is about 20 km. The area of the lake is 2860 hectares, its maximum depth reaches 17 meters [103]. In the west and southeast of the reservoir, the slopes of the mountains are covered with taiga. The bottom of the lake is sandy and pebbly. The shores are mostly flat, sometimes rocky, sometimes sandy. The south-eastern shore is swampy, overgrown with talus, birches, larches. The only river flowing from the lake, the Mazhalyk River, originates here.

Lake Cheder is located 45 km south of the city of Kyzyl, in the south of the Tuva basin in a drainless depression, on board of which the sandy-clay rocks of the Jurassic come out. The depression is surrounded by a hilly, treeless plain. The lake is drainless, located in a shallow depression, within the vast Central Tuva basin, at an absolute mark of 706 m. The lake is fed by a stream flowing into the lake in the southern part, as well as groundwater from quaternary lake sediments. The lake has a slightly elongated shape. The water surface area is 430 ha, length—4.5 km, width—0.8–1.5 km, depth—1.5–1.8 m [119]. The water in the lake is highly mineralized. The main component is sodium sulfate. The mineralization of water in the lake, depending on the level, ranges from 80 in April and May to 200 grams per liter in August. Potassium salts (0.250 g/L), fluorine (0.003 g/L), iodine (0.001 g/L), strontium (0.001 g/L) are present in small quantities. The shores and bottom of the lake are composed of silt mud with a thickness of up to 2 meters. The mud is gray or gray-black with the smell of hydrogen sulfide. On the territory of the lake there is 46-m deep well with mineral drinking water. The mineral water captured by the well is cold, low-mineralized chloride magnesium-sodium-calcium in composition and slightly alkaline in the nature of the reaction of the medium [120].

Thermokarst lakes are located in the Alash Highlands in the Barun-Khemchik district, 6.5 km from the border with Khakassia and 150 km from the city of Ak-Dovurak. Absolute marks in the area of lakes range from 1800 to 2000 m. Absolute heights in the lakes range from 1840 to 1860 m. There are about 200 thermokarst lakes in the study area. Basically, the lakes are small, most of the lakes have a rounded, oval-elongated shape, some of the shores are overgrown and swampy. Two round-shaped lakes were selected for the study.

References

1. Serikova, S.; Pokrovsky, O.; Laudon, H.; Kritskov, I.; Lim, A.G.; Manasypov, R.M.; Karlsson, J. High carbon emissions from thermokarst lakes of Western Siberia. *Nat. Commun.* **2019**, *10*, 1552. [[CrossRef](#)] [[PubMed](#)]
2. Krickov, I.; Lim, A.; Shirokova, L.; Korets, M.; Karlsson, J.; Pokrovsky, O. Environmental controllers for carbon emission and concentration patterns in Siberian rivers during different seasons. *Sci. Total Environ.* **2023**, *859*, 160202. [[CrossRef](#)] [[PubMed](#)]
3. Kirpotin, S.; Antoshkina, O.; Berezin, A.; Elshehawi, S.; Feurdean, A.; Lapshina, E.D.; Pokrovsky, O.S.; Peregon, A.M.; Semenova, N.M.; Tanneberger, F.; et al. Great Vasyugan Mire: How the world's largest peatland helps addressing the world's largest problems. *Ambio* **2021**, *50*, 2038–2049. [[CrossRef](#)] [[PubMed](#)]
4. Chupakov, A.; Pokrovsky, O.; Moreva, O.; Kotova, E.; Vorobyeva, T.Y.; Shirokova, L.S. Export of organic carbon, nutrients and metals by the mid-sized Pechora River to the Arctic Ocean. *Chem. Geol.* **2023**, *632*, 121524. [[CrossRef](#)]
5. Stackpoole, S.; Butman, D.; Clow, D.; Verdin, K.; Gaglioti, B.V.; Genet, H.; Striegl, R.G. Inland waters and their role in the carbon cycle of Alaska. *Ecol. Appl.* **2017**, *27*, 1403–1420. [[CrossRef](#)]

6. Hutchins, R.; Casas-Ruiz, J.; Prairie, Y.; Del Giorgio, P. Magnitude and drivers of integrated fluvial network greenhouse gas emissions across the boreal landscape in Québec. *Water Res.* **2020**, *173*, 115556. [[CrossRef](#)]
7. Pokrovsky, O.; Shirokova, L.; Manasypov, R.; Kirpotin, S.; Kulizhsky, S.; Kolesnichenko, L.; Loiko, S.; Vorobyev, S. Thermokarst lakes of Western Siberia: A complex biogeochemical multidisciplinary approach. *Int. J. Environ. Stud.* **2014**, *71*, 733–748. [[CrossRef](#)]
8. Dristi, A.; Xu, Y.J. Large Uncertainties in CO₂ Water–Air Outgassing Estimation with Gas Exchange Coefficient *K_T* for a Large Lowland River. *Water* **2023**, *15*, 2621. [[CrossRef](#)]
9. Huang, Y.; Zhang, L.; Ran, L. Total Organic Carbon Concentration and Export in a Human-Dominated Urban River: A Case Study in the Shenzhen River and Bay Basin. *Water* **2022**, *14*, 2102. [[CrossRef](#)]
10. Wang, C.; Xv, Y.; Li, S.; Li, X. Interconnected River–Lake Project Decreased CO₂ and CH₄ Emission from Urban Rivers. *Water* **2023**, *15*, 1986. [[CrossRef](#)]
11. Hastie, A.; Lauerwald, R.; Ciais, P.; Regnier, P. Aquatic carbon fluxes dampen the overall variation of net ecosystem productivity in the Amazon basin: An analysis of the interannual variability in the boundless carbon cycle. *Glob. Chang. Biol.* **2019**, *25*, 2094–2111. [[CrossRef](#)] [[PubMed](#)]
12. Moyer, R.; Powell, C.; Gordon, D.; Long, J.; Bliss, C. Abundance, distribution, and fluxes of dissolved organic carbon (DOC) in four small sub-tropical rivers of the Tampa Bay Estuary (Florida, USA). *Appl. Geochem.* **2015**, *63*, 550–562. [[CrossRef](#)]
13. Soria Reinoso, I.; Alcocer, J.; Sánchez-Carrillo, S.; Garcia-Oliva, F.; Cuevas-Lara, D.; Cortes-Guzman, D.; Oseguera, L.A. The Seasonal Dynamics of Organic and Inorganic Carbon along the Tropical Usumacinta River Basin Mexico. *Water* **2022**, *14*, 2703. [[CrossRef](#)]
14. Huang, T.H.; Fu, Y.H.; Pan, P.Y.; Chen, C.T.A. Fluvial carbon fluxes in tropical rivers. *Curr. Opin. Environ. Sustain.* **2012**, *4*, 162–169. [[CrossRef](#)]
15. Galy, A.; Yang, Y.; Fang, X. Sequestration of carbon as carbonate in the critical zone: Insights from the Himalayas and Tibetan Plateau. *Acta Geochim.* **2017**, *36*, 389–391. [[CrossRef](#)]
16. Emberson, R.; Galy, A.; Hovius, N. Weathering of Reactive Mineral Phases in Landslides Acts as a Source of Carbon Dioxide in Mountain Belts. *J. Geophys. Res. Earth Surf.* **2018**, *123*, 2695–2713. [[CrossRef](#)]
17. Ruan, X.; Galy, A. On the significance of periglacial conditions in active mountain belts for chemical weathering processes: Insights from the Chayu area, SE Tibet. *Chem. Geol.* **2021**, *585*, 120581. [[CrossRef](#)]
18. Song, C.; Wang, G.; Hu, Z.; Zhang, T.; Huang, K.; Chen, X.; Li, Y. Net ecosystem carbon budget of a grassland ecosystem in central Qinghai-Tibet Plateau: Integrating terrestrial and aquatic carbon fluxes at catchment scale. *Agric. For. Meteorol.* **2020**, *290*, 108021. [[CrossRef](#)]
19. Song, C.; Wang, G.; Mao, T.; Huang, K.; Sun, X.; Hu, Z.; Chang, R.; Chen, X.; Raymond, P.A. Spatiotemporal variability and sources of DIC in permafrost catchments of the Yangtze River source region: Insights from stable carbon isotope and water chemistry. *Water Resour. Res.* **2020**, *55*, e2019WR025343. [[CrossRef](#)]
20. Wang, L.; Du, Z.; Wei, Z.; Xu, Q.; Feng, Y.; Lin, P.; Lin, J.; Chen, S.; Qiao, Y.; Shi, J.; et al. High methane emissions from thermokarst lakes on the Tibetan Plateau are largely attributed to ebullition fluxes. *Sci. Total Environ.* **2021**, *801*, 149692. [[CrossRef](#)]
21. Zhang, H.; Wang, F.; Shan, S.; Ren, P.; Luo, C.; Fu, W.; Sun, S.; Wang, X. Sources and cycling of dissolved organic and inorganic carbon on the northern Qinghai-Tibetan Plateau: Radiocarbon results from Qinghai Lake. *Sci. Total Environ.* **2022**, *851*, 158123. [[CrossRef](#)] [[PubMed](#)]
22. Zhong, J.; Li, S.L.; Zhu, X.; Jing, L.; Liu, J.; Sen, X.; Sheng, X.; Cong-Qiang, L. Dynamics and fluxes of dissolved carbon under short-term climate variabilities in headwaters of the Changjiang River, draining the Qinghai-Tibet Plateau. *J. Hydrol.* **2021**, *596*, 126128. [[CrossRef](#)]
23. Lin, P.; Du, Z.; Wang, L.; Liu, J.; Xu, Q.; Du, J.; Jiang, R. Hotspots of riverine greenhouse gas (CH₄, CO₂, N₂O) emissions from Qinghai Lake Basin on the northeast Tibetan Plateau. *Sci. Total Environ.* **2023**, *857 Pt 1*, 159373. [[CrossRef](#)] [[PubMed](#)]
24. Kokorin, A. (Ed.) *Assessment Report: Climate Change and Its Impact on Ecosystems, Population and Economy of the Russian Portion of the Altai-Sayan Ecoregion*; WWF Russia: Moscow, Russia, 2011; p. 152.
25. Golubeva, E.; Kerzhentsev, A.; Koropachinsky, I.; Kurbatskaya, S.S.; Pivovarova, Z.F.; Sedelnikov, V.P.; Surov, A.V.; Tebleeva, U.T.; Khakimov, F.I.; Khudyakov, Y.S. *Experiment “Ubsu-Nur”*; Part 1; Intellect: Moscow, Russia, 1995; Volume 1, 336p. (In Russian)
26. Anandhi, A.; Kannan, N. Vulnerability assessment of water resources—Translating a theoretical concept to an operational framework using systems thinking approach in a changing climate: Case study in Ogallala Aquifer. *J. Hydrol.* **2018**, *557*, 460–474. [[CrossRef](#)]
27. Joseph, J.; Ghosh, S.; Pathak, A.; Sahai, A. Hydrologic impacts of climate change: Comparisons between hydrological parameter uncertainty and climate model uncertainty. *J. Hydrol.* **2018**, *566*, 1–22. [[CrossRef](#)]
28. Chaturvedi, A.; Pandey, B.; Yadav, A.; Saroj, S. Chapter 5—An overview of the potential impacts of global climate change on water resources. In *Water Conservation in the Era of Global Climate*; Elsevier: Amsterdam, The Netherlands, 2021; pp. 99–120. [[CrossRef](#)]
29. Chen, Y.; Li, B.; Li, Z.; Li, W. Water resource formation and conversion and water security in arid region of Northwest China. *J. Geogr. Sci.* **2016**, *26*, 939–952. [[CrossRef](#)]
30. Luo, M.; Liu, T.; Meng, F.; Duan, Y.; Bao, A.; Xing, W.; Feng, X.; Maeyer, P.; Frankl, A. Identifying climate change impacts on water resources in Xinjiang, China. *Sci. Total Environ.* **2019**, *676*, 613–626. [[CrossRef](#)]

31. Chen, Z.; Chen, Y.; Li, B. Quantifying the effects of climate variability and human activities on runoff for Kaidu River Basin in arid region of northwest China. *Theor. Appl. Clim.* **2013**, *111*, 537–545. [CrossRef]
32. Kirpotin, S.; Callaghan, T.V.; Peregon, A.; Babenko, A.S.; Berman, D.I.; Bulakhova, N.A.; Byzaakay, A.A.; Chernykh, M.T.; Chursin, V.; Interesoza, E.A.; et al. Impacts of environmental change on biodiversity and vegetation dynamics in Siberia. *Ambio* **2021**, *50*, 1926–1952. [CrossRef]
33. Callaghan, T.; Shaduyko, O.; Kirpotin, S.; Gordov, E. Siberian environmental change: Synthesis of recent studies and opportunities for networking. *Ambio* **2021**, *50*, 2104–2127. [CrossRef]
34. Shukla, P.R.; Skea, J.; Buendía, E.; Masson-Delmotte, V.; Pörtner, H.; Roberts, D.C.; Zhai, P.; Slade, R.; Connors, S.C.; Diemen, S.V.; et al. *IPCC, 2019: Climate Change and Land: An IPCC Special Report on Climate Change, Desertification, Land Degradation, Sustainable Land Management, Food Security, and Greenhouse Gas Fluxes in Terrestrial Ecosystems*; Cambridge University Press: Cambridge, UK; New York, NY, USA, 2019; p. 896. [CrossRef]
35. Shukla, P.R.; Skea, J.; Reisinger, A.; Slade, R.; Fradera, R.; Pathak, M.; Khouradajie, A.A.; Belkacemi, M.; van Diemen, R.; Hasija, A.; et al. *IPCC, 2022: Summary for Policymakers*. In *Climate Change 2022: Mitigation of Climate Change. Contribution of Working Group III to the Sixth Assessment Report of the Intergovernmental Panel on Climate Change*; Cambridge University Press: Cambridge, UK; New York, NY, USA, 2023. [CrossRef]
36. Zalibekov, Z.G. The arid regions of the world and their dynamics in conditions of modern climatic warming. *Arid Ecosyst.* **2011**, *1*, 1–7. [CrossRef]
37. Kulikov, A.I.; Ubugunov, L.L.; Mangataev, A.T. Global climate change and its impact on ecosystems. *Arid Ecosyst.* **2014**, *4*, 135–141. [CrossRef]
38. Berdugo, M.; Delgado-Baquerizo, M.; Soliveres, S.; Hernández-Clemente, R.; Zhao, Y.; Gaitán, J.J.; Gross, N.; Saiz, H.; Maire, V.; Lehmann, A.; et al. Global ecosystem thresholds driven by aridity. *Science* **2020**, *367*, 787–790. [CrossRef] [PubMed]
39. Yao, Y.; Luo, D.; Dai, A.; Simmonds, I. Increased quasi stationarity and persistence of winter Ural blocking and Eurasian extreme cold events in response to Arctic warming. Part I: Insights from observational analyses. *J. Clim.* **2017**, *30*, 3549–3568. [CrossRef]
40. Mokhov, I.I.; Akperov, M.G.; Prokofyeva, M.A.; Timazhev, A.V.; Lupo, A.R.; Treut, H.L. Blockings in the Northern hemisphere and Euro-Atlantic region: Estimates of changes from reanalysis data and model simulations. *Dokl. Earth Sc.* **2013**, *449*, 430–433. [CrossRef]
41. Watanabe, T.; Matsuyama, H.; Kuzhevskaja, I.; Nechepurenko, O.; Chursin, V.; Zemtsov, V. Long-Term Trends of Extreme Climate Indexes in the Southern Part of Siberia in Comparison with Those of Surrounding Regions. *Atmosphere* **2023**, *14*, 1131. [CrossRef]
42. Kattsov, V.M. (Ed.) *The Third Assessment Report on Climate Change and Its Consequences on the Territory of the Russian Federation*; Science-Intensive Technologies: St. Petersburg, Russia, 2022; 676p. (In Russian)
43. Kuular, H.B.O.; Chuldum, A.F.; Hertek, S.B.O.; Namzin, S.A. Spatio-temporal distribution of the spring burnability of the vegetation cover of the Republic of Tyva in 2000–2020. *Nat. Resour. Environ. Soc.* **2021**, *2*, 18–22. (In Russian) [CrossRef]
44. Climate Risk Country Profile: Mongolia (2021): The World Bank Group and the Asian. Available online: <https://www.adb.org/sites/default/files/publication/709901/climate-risk-country-profile-mongolia.pdf> (accessed on 23 July 2023).
45. Adrian, R.; O'Reilly, C.M.; Zagarese, H.; Baines, S.B.; Hessen, D.O.; Keller, W.; Livingstone, D.M.; Sommaruga, R.; Straile, D.; Van Donk, E.; et al. Lakes as sentinels of climate change. *Limnol. Oceanogr.* **2009**, *54*, 2283–2297. [CrossRef]
46. Mladenov, N.; Sommaruga, R.; Morales-Baquero, R.; Laurion, I.; Camarero, L.; Diéguez, M.C.; Camacho, A.; Delgado, A.; Torres, O.; Chen, Z.; et al. Dust inputs and bacteria influence dissolved organic matter in clear alpine lakes. *Nat. Commun.* **2011**, *2*, 405. [CrossRef]
47. Moser, K.A.; Baron, J.S.; Brahney, J.; Oleksy, I.A.; Saros, J.E.; Hundey, E.J.; Sadro, S.A.; Kopáček, J.; Sommaruga, R.; Kainz, M.J.; et al. Mountain lakes: Eyes on global environmental change. *Glob. Planet. Chang.* **2019**, *178*, 77–95. [CrossRef]
48. Rogora, M.; Frate, L.; Carranza, M.L.; Freppaz, M.; Stanisci, A.; Bertani, I.; Bottarin, R.; Brambilla, A.; Canullo, R.; Carbognani, M.; et al. Assessment of climate change effects on mountain ecosystems through a cross-site analysis in the Alps and Apennines. *Sci. Total Environ.* **2018**, *624*, 1429–1442. [CrossRef] [PubMed]
49. Tranvik, L.J.; Downing, J.A.; Cotner, J.B.; Loiselle, S.A.; Striegl, R.G.; Ballatore, T.J.; Dillon, P.; Finlay, K.; Fortino, K.; Knoll, L.B.; et al. Lakes and Reservoirs as Regulators of Carbon Cycling and Climate. *Limnol. Oceanogr.* **2009**, *54*, 2298–2314. [CrossRef]
50. Lehner, B.; Doll, P. Development and validation of a global database of lakes, reservoirs and wetlands. *J. Hydrol.* **2004**, *296*, 1–22. [CrossRef]
51. MacDonald, G.; Edwards, T.; Moser, K.; Pienitz, R.; Smol, J. Rapid response of treeline vegetation and lakes to past climate warming. *Nature* **1993**, *361*, 243–246. [CrossRef]
52. Bunting, L.; Leavitt, P.R.; Weidman, R.P.; Vinebrooke, R.D. Regulation of the Nitrogen Biogeochemistry of Mountain Lakes by Subsidies of Terrestrial Dissolved Organic Matter and the Implications for Climate Studies. *Limnol. Oceanogr.* **2010**, *55*, 333–345. Available online: <http://www.jstor.org/stable/20622883> (accessed on 23 September 2023). [CrossRef]
53. Oidup, C.K. Lithium-uranium mineralization of salt lakes and underground springs of Central Tuva. *Geospheric. Res.* **2018**, *3*, 22–33. [CrossRef]
54. Kyzyl, O.M. Hydrogeochemistry of mineral water sources of the Republic of Tyva. *Bull. Kurgan State Univ.* **2015**, *4*, 2222–3371. Available online: <https://cyberleninka.ru/article/n/gidrogeohimiya-mineralnyh-istochnikov-vod-respubliki-tyva> (accessed on 18 March 2023). (In Russian)

55. Yu, I.K.; Khvashchevskaya, A.A. Features of the chemical composition of groundwater springs of Western Tuva. *Resort Base Nat. Health-Impr. Areas Tuva Adjac. Reg.* **2015**, *2*, 167–173. (In Russian)
56. Kalnaya, O.I.; Rychkova, O.I.; Ayunova, O.D.; Archimaeva, T.P. Ecological and hydrochemical state of watercourses in the area of Kyzyl (Republic of Tyva). *Nat. Resour. Environ. Soc.* **2020**, *4*, 52–60. (In Russian)
57. Kalnaya, O.I.; Ainova, O.D. Retrospective analysis of the ecological and hydrochemical state of two-dimensional and auxiliary means in the region of Lake Duskhol (Svatikovo), central Tuva. *Nat. Resour. Environ. Soc.* **2022**, *1*, 37–47. (In Russian)
58. Kirova, N.A.; Kalnaya, O.I.; Ayunova, O.D. On the Issue of Hydrochemistry and Biology of Lake Duskhol (Tuva). *Izv. AO RGO* **2018**, 82–88. Available online: <https://cyberleninka.ru/article/n/k-voprosu-o-gidrohimii-i-biologii-ozera-dus-hol-tuva>. (accessed on 20 March 2023). (In Russian)
59. Sambuu, A.; Ayunova, O.; Chupikova, S.; Dugerzhaa, C.S.; Biche-ool, O.E. Water resources of the republic of Tuva and their current state. *Int. J. Hydrol. Sci. Technol.* **2020**, *7*, 60–66. (In Russian) [CrossRef]
60. State Report “On the State and Environmental Protection of the Republic of Tyva in 2019”—Text: Electronic//Ministry of Natural Resources and Ecology of the Republic of Tyva: Official Website. 2019. Available online: <https://mpr.rtyva.ru/upload/files/f992a01d-bc33-488f-8f71-ea266cfa02ec.pdf> (accessed on 14 February 2023). (In Russian)
61. Chupikova, S.A.; Prudnikov, S.D.; Chuldum, A.F. Morphometric analysis of the water intake of relig-Hem (Tuva) using GIS and DDZ. *Bull. SGUGiT (Sib. State Geosystem Univ. Technol. Univ.)* **2023**, *28*, 76–88. (In Russian)
62. Mineeva, L.A.; Arakchaa, K.K.D.; Kyzyl, O.M. Physical and chemical characteristics of mineral waters from the Shumak and Choigan deposits. *Bull. Irkutsk. State Univ. Ser. Earth Sci.* **2016**, *17*, 115–134. (In Russian)
63. Kopylova, Y.G.; Guseva, N.V.; Arakchaa, K.D.; Khvashchevskaya, A.A. Geochemistry of carbon dioxide mineral waters of the Choigan natural complex (northeastern Tuva). *Russ. Geol. Geophys.* **2014**, *55*, 1295–1305. [CrossRef]
64. Sodnam, N.I.; Kashkak, E.S.; Oorzhak, U.S. Physico-chemical review of arzhanov Ovyursky district. *Bull. Tuva State Univ. Nat. Agric. Sci.* **2019**, *2*, 52–58. (In Russian)
65. Klopotova, N.G.; Sidorina, N.G. The current state and study of therapeutic hydromineral resources of Tuva. *Resort Base Nat. Health-Impr. Areas Tuva Adjac. Reg.* **2013**, *1*, 16–19. (In Russian)
66. Szopińska, M.; Szumińska, D.; Polkowska, Ż.; Machowiak, K.; Lehmann, S.; Chmiel, S. The chemistry of river-lake systems in the context of permafrost occurrence (Mongolia, Valley of the Lakes). Part, I. Analysis of ion and trace metal concentrations. *Sediment. Geol.* **2016**, *340*, 74–83. [CrossRef]
67. Kuular, H.B. Climate warming in the Republic of Tyva according to ground observations. *Nat. Resour. Environ. Soc.* **2021**, *1*, 62–67. (In Russian) [CrossRef]
68. Arakchaa, K.D. Prospects for the development of balneoresources of lake Cheder. *Nat. Resour. Environ. Soc.* **2021**, *1*, 21–29. Available online: <https://cyberleninka.ru/article/n/perspektivy-osvoeniya-balneoresurov-ozera-cheder> (accessed on 23 September 2023). (In Russian)
69. Dubovik, D.S.; Yakutin, M.V. The use of Earth remote sensing data in monitoring of small lakes of the Ubsunur basin (Tyva). *Interexpo Geo-Sib.* **2016**, *4*, 74–78.
70. Johnson, M.S.; Billett, M.F.; Dinsmore, K.J.; Wallin, M.B.; Dyson, K.E.; Jassal, R.S. Direct and continuous measurement of dissolved carbon dioxide in freshwater aquatic systems—Method and applications. *Ecolhydrology* **2010**, *3*, 68–78. [CrossRef]
71. Kuhn, M.; Lundin, E.J.; Giesler, R.; Johansson, M.; Karlsson, J. Emissions from thaw ponds largely offset the carbon sink of northern permafrost wetlands. *Sci. Rep.* **2018**, *8*, 9535. [CrossRef] [PubMed]
72. Lim, A.; Kritskov, I.; Vorobyev, S.; Korets, M.; Kopysov, S.; Shirokova, L.S.; Karlsson, J.; Pokrovsky, O.S. Carbon emission and export from the Ket River, western Siberia. *Biogeosciences* **2022**, *19*, 5859–5877. [CrossRef]
73. Krickov, I.; Serikova, S.; Pokrovsky, O.; Vorobyev, S.N.; Lim, A.G.; Siewert, M.B.; Karlsson, J. Sizable carbon emission from the floodplain of Ob River. *Ecol. Indic.* **2021**, *131*, 108164. [CrossRef]
74. Vorobyev, S.N.; Karlsson, J.; Kolesnichenko, Y.Y.; Korets, M.A.; Pokrovsky, O.S. Fluvial carbon dioxide emission from the Lena River basin during the spring flood. *Biogeosciences* **2021**, *18*, 4919–4936. [CrossRef]
75. Zabelina, S.; Shirokova, L.; Klimov, S.; Chupakov, A.; Lim, A.; Polishchuk, Y.M.; Polishchuk, V.Y.; Bogdanov, A.N.; Muratov, I.N.; Guerin, F.; et al. Carbon emission from thermokarst lakes in NE European tundra. *Limnol. Oceanogr.* **2020**, *66*, S216–S230. [CrossRef]
76. Drozdova, O.Y.; Ilina, S.M.; Anokhina, N.A.; Zavgorodnyaya, Y.A.; Demin, V.V.; Lapitskiy, S.A. Organic Matter Transformation in the Conjugate Series of Surface Water in Northern Karelia. *Water Resour.* **2019**, *46*, 52–58. [CrossRef]
77. Ilina, S.M.; Drozdova, O.Y.; Lapitskiy, S.A.; Alekhin, Y.V.; Demin, V.; Zavgorodnyaya, Y.; Shirokova, L.; Viers, J.; Pokrovsky, O.S. Size fractionation and optical properties of dissolved organic matter in the continuum soil solution-bog-river and terminal lake of a boreal watershed. *Org. Geochem.* **2014**, *66*, 14–24. [CrossRef]
78. Jaffé, R.; Boyer, J.N.; Lu, X.; Maie, N.; Yang, C.; Scully, N.M.; Mock, S. Source characterization of dissolved organic matter in a subtropical mangrove-dominated estuary by fluorescence analysis. *Mar. Chem.* **2004**, *84*, 195–210. [CrossRef]
79. Battin, T.J. Dissolved organic materials and its optical properties in a blackwater tributary of the upper Orinoco River, Venezuela. *Org. Geochem.* **1998**, *28*, 561–569. [CrossRef]
80. Li, M.; Peng, C.; Wang, M.; Xue, W.; Zhang, K.; Wang, K.; Shi, G.; Zhu, Q. The carbon flux of global rivers: A re-evaluation of amount and spatial patterns. *Ecol. Indic.* **2017**, *80*, 40–51. [CrossRef]

81. Cole, J.J.; Prairie, Y.T.; Caraco, N.F.; McDowell, W.H.; Tranvik, L.J.; Striegl, R.G.; Duarte, C.M.; Kortelainen, P.; Downing, J.A.; Middelburg, J.J.; et al. Plumbing the Global Carbon Cycle: Integrating Inland Waters into the Terrestrial Carbon Budget. *Ecosystems* **2007**, *10*, 172–185. [[CrossRef](#)]
82. Raymond, P.; Hartmann, J.; Lauerwald, R.; Lauerwald, R.; Sobek, S.; McDonald, C.; Hoover, M.; Butman, D.; Striegl, R.; Mayorga, E.; et al. Global carbon dioxide emissions from inland waters. *Nature* **2013**, *503*, 355–359. [[CrossRef](#)] [[PubMed](#)]
83. Kirpotin, S.N.; Kvasnikova, Z.N.; Potapova, S.A.; Volkova, I.I.; Volkov, I.V.; Pyak, A.I.; Byzaakay, A.A.; Kolesnichenko, L.G.; Lushchaeva, I.V.; Khovalyg, A.O.; et al. Pilot Studies of the Unique Highland Palsa Mire in Western Sayan (Tuva Republic, Russian Federation). *Atmosphere* **2022**, *13*, 32. [[CrossRef](#)]
84. Pokrovsky, O.S.; Viers, J.; Dupre, B.; Chabaux, F.; Gaillardet, J.; Audry, S.; Prokushkin, A.S.; Shirokova, L.S.; Kirpotin, S.N.; Lapitsky, S.A.; et al. Biogeochemistry of carbon, major and trace elements in watersheds of Northern Eurasia drained to the Arctic Ocean: The change of fluxes, sources and mechanisms under the climate warming prospective. *Comptes Rendus Geosci.* **2012**, *344*, 663–677. [[CrossRef](#)]
85. Krickov, I.; Lim, A.G.; Loiko, S.V.; Vorobyev, S.N.; Shevchenko, V.P.; Dara, O.M.; Gordeev, V.V.; Pokrovsky, O.S. Major and trace elements in suspended matter of western Siberian rivers: First assessment across permafrost zones and landscape parameters of watersheds. *Geochim. Cosmochim. Acta* **2020**, *269*, 429–450. [[CrossRef](#)]
86. Bagard, M.L.; Chabaux, F.; Stille, P.; Rihs, S.; Pokrovsky, O.S.; Viers, J.; Dupré, B.; Prokushkin, A.S.; Schmitt, A.D. Seasonal variability of element fluxes in two Central Siberian rivers draining high latitude permafrost dominated areas. *Geochim. Cosmochim. Acta* **2011**, *75*, 3335–3357. [[CrossRef](#)]
87. Manasypov, R.M.; Vorobyev, S.N.; Loiko, S.V.; Kritzkov, I.V.; Kirpotin, S.N.; Kulizhsky, S.P.; Kolesnichenko, L.G.; Zemtsov, V.A.; Sinkin, V.V.; Pokrovsky, O.S.; et al. Seasonal dynamics of organic carbon and metals in thermokarst lakes from the discontinuous permafrost zone of western Siberia. *Biogeosciences* **2015**, *12*, 3009–3028. [[CrossRef](#)]
88. Frey, K.E.; McClelland, J.W. Impacts of permafrost degradation on arctic river biogeochemistry. *Hydrol. Process.* **2009**, *23*, 169–182. [[CrossRef](#)]
89. Calabrese, S.; Parolari, A.J.; Porporato, A. Hydrologic Transport of Dissolved Inorganic Carbon and Its Control on Chemical Weathering. *J. Geophys. Res. Earth Surf.* **2017**, *122*, 2016–2032. [[CrossRef](#)]
90. Park, S.; Joe, K.S.; Han, S.H.; Kim, H.S. Characteristics of dissolved organic carbon in the leachate from Moonam Sanitary Landfill. *Environ. Technol.* **1999**, *20*, 419–424. [[CrossRef](#)]
91. Hutchins, R.H.S.; Aukes, P.; Schiff, S.L.; Dittmar, T.; Prairie, Y.T.; del Giorgio, P.A. The optical, chemical, and molecular dissolved organic matter succession along a boreal soil-stream-river continuum. *J. Geophys. Res. Biogeosci.* **2017**, *122*, 2892–2908. [[CrossRef](#)]
92. Shirokova, L.S.; Pokrovsky, O.S.; Kirpotin, S.N.; Desmukh, C.; Pokrovsky, B.G.; Audry, S.; Viers, J. Biogeochemistry of organic carbon, CO₂, CH₄, and trace elements in thermokarst water bodies in discontinuous permafrost zones of Western Siberia. *Biogeochemistry* **2013**, *113*, 573–593. [[CrossRef](#)]
93. Payandi-Rolland, D.; Shirokova, L.S.; Nakhle, P.; Tesfa, M.; Abdou, A.; Causserand, C.; Lartiges, B.; Rols, J.-L.; Guerin, F.; Benezeth, P.; et al. Aerobic release and biodegradation of dissolved organic matter from frozen peat: Effects of temperature and heterotrophic bacteria. *Chem. Geol.* **2020**, *536*, 119448. [[CrossRef](#)]
94. Payandi-Rolland, D.; Shirokova, L.S.; Lariux, J.; Bénézech, P.; Pokrovsky, O.S. Laboratory growth capacity of an invasive cyanobacterium (*Microcystis aeruginosa*) on organic substrates from surface waters of permafrost peatlands. *Environ. Sci. Process. Impacts* **2023**, *25*, 659–669. [[CrossRef](#)]
95. Jia, J.; Sun, K.; Lu, S.; Li, M.; Wang, Y.; Yu, G.; Gao, Y. Determining whether Qinghai–Tibet Plateau waterbodies have acted like carbon sinks or sources over the past 20 years. *Sci. Bull.* **2022**, *67*, 2345–2357. [[CrossRef](#)] [[PubMed](#)]
96. Wang, L. In-situ measurement on air–water flux of CH₄, CO₂ and their carbon stable isotope in lakes of northeast Tibetan Plateau. *Adv. Clim. Chang. Res.* **2022**, *13*, 279–289. [[CrossRef](#)]
97. Yu, C.; Li, Y.; Jin, H.; Ma, Q.; Yu, Z.; Shi, K.; Li, X.; Chen, G. Organic versus Inorganic Carbon Exports from Glacier and Permafrost Watersheds in Qinghai–Tibet Plateau. *Aquat. Geochem.* **2021**, *27*, 283–296. [[CrossRef](#)]
98. Maurischat, P.; Lehnert, L.; Zerres, H.D.V.; Tran, T.V.; Kalbitz, K.; Rinnan, Å.; Li, X.G.; Dorji, T.; Guggenberger, G. The glacial–terrestrial–fluvial pathway: A multiparametrical analysis of spatiotemporal dissolved organic matter variation in three catchments of Lake Nam Co, Tibetan Plateau. *Sci. Total Environ.* **2022**, *838*, 156542. [[CrossRef](#)]
99. Jin, Z.D.; You, C.F.; Wang, Y.; Shi, Y. Hydrological and solute budgets of Lake Qinghai, the largest lake on the Tibetan Plateau. *Quat. Int.* **2010**, *218*, 151–156. [[CrossRef](#)]
100. Xie, J.X.; Li, Y.; Zhai, C.X.; Li, C.; Lan, Z. CO₂ absorption by alkaline soils and its implication to the global carbon cycle. *Environ. Geol.* **2009**, *56*, 953–961. [[CrossRef](#)]
101. Golubyatnikov, L.; Kurganova, I.N.; de Gerenyu, V.L. Estimation of C–CO₂ balance of natural steppe ecosystems: Khakassia and Tuva (Eastern Siberia, Russia) case studies. *IOP Conf. Ser. Earth Environ. Sci.* **2020**, *606*, 012013. [[CrossRef](#)]
102. Karlsson, J.; Serikova, S.; Rocher-Ros, G.; Denfeld, B.; Vorobyev, S.N.; Pokrovsky, O.S. Carbon emission from Western Siberian inland waters. *Nat. Commun.* **2021**, *12*, 825. [[CrossRef](#)] [[PubMed](#)]
103. Karabaeva, L. *Surface Water Resources of the USSR: Hydrological Knowledge. Angaro-Yenisei District. Question 1. Yenisei*; Hydrometeoizdat: Leningrad, Russia, 1973; Volume 16, p. 823.
104. State Report on the State and Environmental Protection of the Republic of Tyva in 2018. Available online: <http://docs.cntd.ru/document/561543920> (accessed on 25 December 2022).

105. Grebneva, V.A. *Geography of the Tuva ASSR*; Tuva Book Publishing House: Gaithersburg, MD, USA, 1972; Volume 2, 132p.
106. Ochur-ool, A.O. Ecological and Geochemical State of the Landscapes of the Khemchik Basin (Western Tyva). Ph.D. Thesis, Candidate of Geographical Sciences, Kyzyl-Tomsk, Russia, 2016; 175p. Available online: <https://vital.lib.tsu.ru/vital/access/services/Download/vtls:000563256/SOURCE1> (accessed on 18 June 2023).
107. Makarieva, O.M.; Nesterova, N.V.; Yampolsky, G.P.; Kudymova, E.Y.; Ostashov, A.A.; Kolupaeva, A.D. The Oenc is a maximum category of aqueducts of versatile observation and unexplored mountain river Khemchik (Republic of Tyva) based on mathematical modeling methods. *Eng. Surv.* **2019**, *XIII*, 36–51. [CrossRef]
108. State Water Register: Alash River. Available online: <https://textual.ru/gvr/index.php?card=212139> (accessed on 15 August 2023).
109. State Water Register: Ak-Sug River. Available online: <https://textual.ru/gvr/index.php?card=211467> (accessed on 17 August 2023).
110. Potapova, S.A. Analysis of the physical and geographical conditions of the Ak-Sug river basin as a stage of monitoring vulnerable ecosystems of the Republic of Tuva/Geographical studies of Siberia and the Altai-Sayan transboundary region. In Proceedings of the International Scientific and Practical Conference, Veliky Novgorod, Russia, 28–29 June 2021; pp. 423–434.
111. Chadan River: According to the State Water Register. Available online: <http://www.textual.ru/gvr/index.php?card=212241> (accessed on 20 August 2023).
112. Khayan, A.B. Geocological state of the Durgen river. Ecology of Southern Siberia and adjacent territories. In Proceedings of the Conference “Ecological Siberia and the Limit of Territories”; 2014; pp. 154–155. Available online: <https://www.elibrary.ru/item.asp?id=23627503> (accessed on 4 February 2023).
113. Nazyn, C.D. The first information about the algae of the Torgalyg River (Tuva, Russia). *Resort Base Nat. Health-Improv. Areas Tuva Adjac. Reg.* **2013**, 189–192. (In Russian)
114. State Water Register: Anyak-Chyrgaki River. Available online: <https://textual.ru/gvr/index.php?card=212216> (accessed on 14 December 2021).
115. State Water Register: Biche-Bayan-Kol River. Available online: <https://textual.ru/gvr/index.php?card=212200> (accessed on 14 December 2021).
116. Alash Plateau: The Great Soviet Encyclopedia. Available online: <https://bio.1sept.ru/article.php?ID=200203204> (accessed on 18 August 2023).
117. Shilkrot, G.S.; Kretova, S.P.; Smirnova, E.V. Ecosystem of Lake Ubsu-Nur potential and water quality. Informational problems of studying the biosphere. *Pushchino* **1990**, 236–303.
118. Protected Areas of Russia: Lake Tore-Khol. Available online: <http://oopt.aari.ru/oopt/%D0%9E%D0%B7%D0%B5%D1%80%D0%BE%D0%A2%D0%BE%D1%80%D0%B5-%D0%A5%D0%BE%D0%BB%D1%8C> (accessed on 20 December 2021).
119. Protected Areas of Russia: Lake Cheder. Available online: <http://oopt.aari.ru/oopt/%D0%9E%D0%B7%D0%B5%D1%80%D0%BE-%D0%A7%D0%B5%D0%B4%D0%B5%D1%80> (accessed on 16 August 2023).
120. Erdynieva, L.S. Use of Natural and Ecological Resources of Lake Cheder. The World of Science, Culture, Enlightenment 2010. pp. 312–315. Available online: <https://cyberleninka.ru/article/n/ispolzovanie-prirodno-ekologicheskikh-resursov-ozera-cheder> (accessed on 20 May 2023).

Disclaimer/Publisher’s Note: The statements, opinions and data contained in all publications are solely those of the individual author(s) and contributor(s) and not of MDPI and/or the editor(s). MDPI and/or the editor(s) disclaim responsibility for any injury to people or property resulting from any ideas, methods, instructions or products referred to in the content.